

Solubilizing core modifications on high-performing benzodithiophene-based molecular semiconductors and their influences on film nanostructure and photovoltaic performance

*Calvin J. Lee, Valerie D. Mitchell, Jonathan White, Xuechen Jiao, Christopher R. McNeill,
Jegadesan Subbiah and David J. Jones **

S1 Materials and Methods

Unless noted, all materials were reagent grade and used as received without further purification. Anhydrous solvents were prepared by drying HPLC grade solvents using freshly activated molecular sieves. Chromatographic separations were performed using standard column methods with silica gel (Merck 9385 Kieselgel). Thin layer chromatography was performed on Merck Kieselgel 60 silica gel on glass (0.25 mm thick).

IR spectra were obtained on a Perkin Elmer Spectrum One FT-IR spectrometer and UV-vis spectra were recorded using a Cary 50 UV-Vis spectrometer. Photoluminescence was measured with a Varian Cary Eclipse fluorimeter. ^1H NMR and ^{13}C NMR spectra were carried out on a 400 MHz or 600 MHz spectrometer. All NMR data was referenced to the chloroform signal and peak multiplicity was reported as follows: s = singlet, d = doublet, t = triplet, q = quartet, p = pentet, dd = doublets of doublets, m = multiplet). MALDI-TOF mass spectrometry was performed on a Bruker microflex instrument, using chloroform as solvent and DCTB or terthiophene as the assisted matrix.

Elemental analyses were obtained commercially through Chemical & Analytical Services Pty. Ltd. (Australia) an Exeter Analytical CE-440 elemental analyzer. Thermal gravimetric analysis (TGA) experiments were carried out with a Mettler Toledo TGA/SDTA851e and differential scanning calorimetry (DSC) experiments were performed on a Perkin-Elmer Sapphire DSC at a ramp rate of $10\text{ }^\circ\text{C min}^{-1}$.

Cyclic voltammetry (CV) experiments were performed at a sweep rate of 100 mV/s. CVs were carried out in a three-electrode cell consisting of a glassy carbon working electrode, a platinum wire auxiliary electrode, and an Ag/Ag⁺ pseudo-reference electrode. The supporting electrolyte was 0.10 M tetrabutylammonium hexafluorophosphate (Bu₄NPF₆) in CH₃CN. The solutions were deoxygenated by sparging with argon prior to each scan and blanketed with argon during the scans. The glassy carbon working electrode was prepared by polishing with 5 mm alumina and washed and dried before the polymer was drop-casted on the electrode from chlorobenzene solution to form a film. Ferrocene/ferrocenium redox couple was used as the internal standard.

CCDC 1864646 contains the supplementary crystallographic data for this paper. This data can be obtained free of charge from The Cambridge Crystallographic Data Centre via www.ccdc.cam.ac.uk/data_request/cif.

S1.1 Device fabrication and characterization:

Organic photovoltaic devices were processed on pre-patterned indium tin oxide (ITO)coated glass substrates with a sheet resistance of 15 Ω per square. The conventional devices were fabricated with a device geometry of glass/ITO/PEDOT:PSS/active layer/Ca/Al. The ITO-coated glass substrates were cleaned by ultrasonic treatment in acetone and isopropyl alcohol for 15 minutes each and subsequently treated in UV–Ozone for 15 minutes. A thin layer of MoO₃/V₂O₅ was spin-coated onto the ITO surface. After being baked at 150 °C for 10 minutes, the substrates were transferred into a nitrogen-filled glove box. Subsequently, the active layer was spin-coated from blend chloroform solutions (32 mg/mL) with weight ratio of BTR analogue and PC₇₁BM at 1:1 and the active layer thicknesses of all films were measured as 210–260 nm. Then, the substrates were placed in a glass Petri dish containing 1 mL THF or CHCl₃ for solvent vapour annealing (SVA), as specified in the main body of the text. After SVA treatment, the films were transferred to a metal evaporation chamber and a bilayer cathode

consisted of Ca (30 nm) capped with Al (100 nm) was deposited through a shadow mask (active area was 0.1 cm²) at approximately 1×10^{-6} Torr.

S1.2 Thin-film fabrication and characterization:

Samples were prepared for GIWAXS by spin-coating solutions of BTR analogue blends onto PEDOT:PSS coated Si substrates using the same deposition condition and annealing conditions as for the photovoltaic devices. The Si wafers had been sonicated in acetone and isopropanol for 30 minutes each followed by 15 minutes of UV/Ozone treatment. GIWAXS experiments were performed at the Australian Synchrotron on the SAXS/WAXS beamline under ambient conditions. A Pilatus 200K detector was used for 2D diffraction pattern collection. The energy of the incident beam was 11 kEV at a range of incident angles from $\theta = 0.02 - 0.20^\circ$. The sample-to-detector range was 28 cm. Data from GIWAXS experiments was gathered from the SAXS/WAXS beamline of the Australian Synchrotron and analysed using a customized version of NIKA 2D based in IgorPro.^[1] Single-crystal data was gathered from the MX1 beamline at the Australian Synchrotron^[2] Atomic force microscopy images were acquired using an Asylum Research Cypher scanning probe microscope operated in tapping mode.

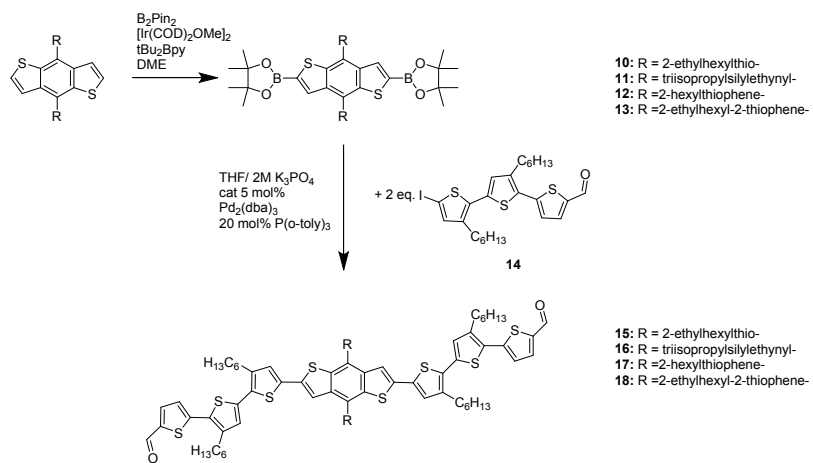
S1.3 Space charge limite current measurements:

The space charge limited current (SCLC) of molecular semiconductors (BTR-TIPS/BTR-TE/BTE-EH/H) were studied using hole-only devices to find the charge-transport properties. The hole-only devices, consisting of active layer sandwiched between a PEDOT:PSS coated ITO electrode and Au counter-electrode as the electron-blocking contact, were fabricated as shown in figure S1. From the current density as a function of voltage data, the hole mobility in the space-charge limited current (SCLC) region can be estimated using the Mott-Gurney equation, $J=9(\epsilon_r\epsilon_0\mu)/8 \times (V^2/d^3)$, where J is the current density, V = V_{appl} – V_{bi}, V_{appl} is the applied potential, V_{bi} is the built-in potential resulting from workfunction difference between two electrodes, ϵ_r is the dielectric constant of molecular semiconductor, ϵ_0 is the permittivity of vacuum, μ is the hole mobility, d is the sample thickness.

S2 Synthesis

The synthesis of the thioester-functionalized BDT core (compounds **1-6**),^[3] the triisopropylsilylethyynyl-functionalized BDT core (compound **7**)^[4], the 2-hexylthienyl functionalized BDT core (compound **8**)^[5] and the 2-(2'-ethylhexyl)thienyl functionalized BDT core (compound **9**)^[6] have all previously been reported in the literature. Synthesis of the terthiophene π -bridge (compound **14**) and the n-hexyl rhodanine acceptor (compound **19**) has been reported in our earlier work.^[7]

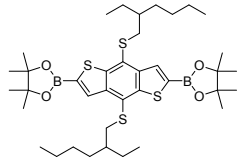
S2.1 General synthesis of BTR-Dialdehyde cores



General procedure for the diborylated BDT cores

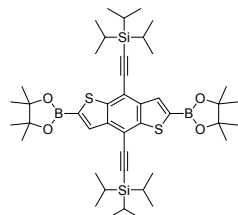
To a Schlenk flask was added the corresponding BDT core (1 g), B_2Pin_2 (1.5 eq.), bis-*tert*-butylbipyridine (0.06 eq.) and $[\text{Ir}(\text{COD})\text{OMe}]_2$ (0.02 eq.) and the flask heated under vacuum for 1 hour at 60°C. Dry, degassed DME (2 mL) was added and the temperature raised to 85 °C. The reaction was stirred for 2 hours under N_2 after which the reaction vessel was cooled to RT. The crude mixture was precipitated in IPA and the product collected via filtration, and after drying under vacuum, yielded analytically pure material.

S2.1.1 *2,2'-(4,8-bis((2-ethylhexyl)thio)benzo[1,2-b:4,5-b']dithiophene-2,6-diyl)bis(4,4,5,5-tetramethyl-1,3,2-dioxaborolane) (10)*



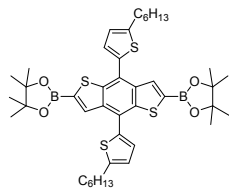
Product formed light brown crystals. Yield = 1.3 g (1.78 mmol, 85%). ^1H NMR (400 MHz, CDCl_3) δ 8.28 (s, 2H), 3.00 (d, J = 4.9 Hz, 4H), 1.55 (s, CH_3 , 12H), 1.47-1.15 (m, 18H), 0.82 (m, 12H). ^{13}C NMR (125 MHz, CDCl_3) δ 148.00, 142.03, 134.25, 124.59, 84.56, 40.28, 39.99, 32.10, 28.77, 25.48, 24.81, 22.90, 14.06, 10.75. IR (Neat): ν = 2958, 2923, 2856, 2298, 2160, 1536, 1321, 1134, 848, 662 cm^{-1} . MS(MALDI $^+$) m/z calculated for $\text{C}_{38}\text{H}_{60}\text{B}_2\text{O}_4\text{S}_4[\text{M}^+]$: 730.36, found: 730.47. Elemental analysis calculated for $\text{C}_{38}\text{H}_{60}\text{B}_2\text{O}_4\text{S}_4$: C, 62.46; H, 8.28; B, 2.96; O, 8.76; S, 17.55. Found: C, 62.39; H, 8.47; N: 0.00

S2.1.2 *((2,6-bis(4,4,5,5-tetramethyl-1,3,2-dioxaborolan-2-yl)benzo[1,2-b:4,5-b']dithiophene-4,8-diyl)bis(ethyne-2,1-diyl))bis(triisopropylsilane) (11)*



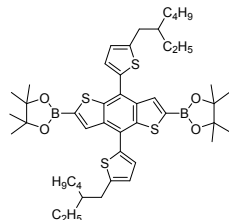
Product formed bright yellow crystals. Yield = 1.03 g, (1.29 mmol, 71%). ^1H NMR (600 MHz, CDCl_3) δ 8.11 (s, 2H), 1.39 (s, 24H), 1.23 (s, 36H). ^{13}C NMR (125 MHz, CDCl_3) δ 144.26, 140.16, 133.50, 112.66, 102.46, 102.12, 84.57, 24.80, 18.82, 11.34, 11.30. IR (Neat): ν = 2940, 2889, 2863, 2229, 2065, 1460, 880, 662 cm^{-1} . MS(MALDI $^+$) m/z calculated for $\text{C}_{44}\text{H}_{68}\text{B}_2\text{O}_4\text{S}_2\text{Si}_2$ [M $^+$]: 802.43, found: 802.56. Elemental analysis calculated for $\text{C}_{44}\text{H}_{68}\text{B}_2\text{O}_4\text{S}_2\text{Si}_2$: C:65.82; H, 8.54; B, 2.69; O, 7.97; S, 7.99; Si, 7.00. Found: C:65.69; H, 8.26; N: 0.00

S2.1.3 *2,2'-(4,8-bis(5-hexylthiophen-2-yl)benzo[1,2-b:4,5-b']dithiophene-2,6-diyl)bis(4,4,5,5-tetramethyl-1,3,2-dioxaborolane)* (**12**)



Product formed bright yellow crystals. Yield = 1.14 g, (1.47 mmol, 85%). ^1H NMR (400 MHz, CDCl_3) δ 8.12 (s, 2H), 7.26 (d, J = 3.0 Hz, 2H), 6.87 (d, J = 3.4 Hz, 2H), 2.90 (t, J = 7.7 Hz, 4H), 1.84 – 1.69 (m, 4H), 1.46 (s, 4H), 1.35 (s, 24H), 0.94 (d, J = 6.9 Hz, 6H). ^{13}C NMR (125 MHz, CDCl_3) δ 147.20, 142.60, 138.31, 136.59, 133.61, 128.09, 124.80, 124.25, 84.50, 31.60, 30.25, 28.96, 24.77, 22.60, 14.11. IR (Neat): ν = 2929, 2854, 2029, 1533, 1424, 1328, 1137, 849, 665 cm^{-1} . MS(MALDI $^+$) m/z calculated for $\text{C}_{42}\text{H}_{56}\text{B}_2\text{O}_4\text{S}_4$ [M $^+$]: 774.77, found: 774.49. Elemental analysis calculated for $\text{C}_{42}\text{H}_{56}\text{B}_2\text{O}_4\text{S}_4$: C, 65.11; H, 7.29; B, 2.79; O, 8.26; S, 16.55. Found: C, 66.08; H, 7.47; N: 0.00

S2.1.4 *2,2'-(4,8-bis(5-(2-ethylhexyl)thiophen-2-yl)benzo[1,2-b:4,5-b']dithiophene-2,6-diyl)bis(4,4,5,5-tetramethyl-1,3,2-dioxaborolane)* (**13**)



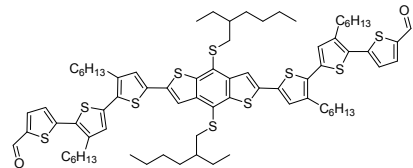
Product formed bright yellow crystals. Yield = 1.16 g (1.40 mmol, 81%). ^1H NMR (600 MHz, CDCl_3) δ 8.14 (s, 2H), 7.28 (d, J = 3.4 Hz, 2H), 6.85 (d, J = 3.5 Hz, 2H), 2.84 (d, J = 6.7 Hz, 4H), 1.67 (d, J = 6.3 Hz, 2H), 1.35 (s, 40H), 1.01 – 0.82 (m, 12H). ^{13}C NMR (125 MHz, CDCl_3) δ 145.80, 142.56, 138.25, 136.86, 133.64, 128.02, 125.32, 124.78, 84.48, 41.38, 34.25, 32.46, 30.89, 28.93, 25.66, 24.75, 23.01, 14.16, 10.84. IR (Neat): ν = 2929, 2854, 2029, 1533, 1424, 1328, 1137, 849, 665 cm^{-1} . MS(MALDI $^+$) m/z calculated for $\text{C}_{46}\text{H}_{64}\text{B}_2\text{O}_4\text{S}_4$ [M $^+$]: 830.39,

found: 830.61. Elemental analysis calculated for C₄₆H₆₄B₂O₄S₄: 66.49; H, 7.76; B, 2.60; O, 7.70; S, 15.44. Found; C:66.25; H, 7.71; N: 0.00

General procedure for the BTR dialdehydes

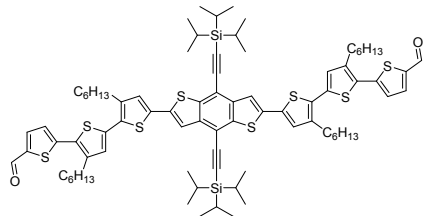
A mixture of the borylated BDT core (0.5 g), 3',3"-dibutyl-5"-ido-[2,2':5',2"-terthiophene]-5-carbaldehyde **14** (2.2 eq.), THF (30 mL) and 2.0 M K₃PO₄ (15 mL) was degassed by bubbling dinitrogen through for 30 minutes. The catalyst, Pd₂(dba)₃ (5 mol%) and P(*o*-tol)₃ (20 mol%) was added and the reaction mixture was stirred at 60°C for 12 h. The reaction mixture was filtered through celite filter aid and the THF removed under vacuum. Diethyl ether (40 mL) was added and the organic phase separated, washed with water (2 x 20 mL) and dried over MgSO₄ and filtered. After removing the solvent the crude product was purified by silica gel column chromatography (petroleum spirit: dichloromethane = 1:1) to give the pure product.

*S2.1.5 Synthesis of 5",5'''-(4,8-bis((2-ethylhexyl)thio)benzo[1,2-*b*:4,5-*b*']dithiophene-2,6-diyl)bis(3',3"-dihexyl-[2,2':5',2"-terthiophene]-5-carbaldehyde) (**15**)*



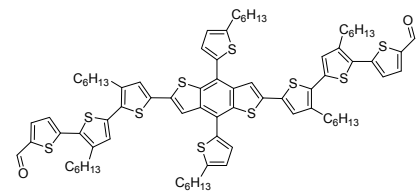
Product formed a red powder. Yield = 0.69 g, (0.51 mmol, 74%). R_f = 0.20 (PS:DCM = 1:1) ¹H NMR (600 MHz, CDCl₃) δ 9.89 (s, 2H), 7.71 (d, *J* = 1.5 Hz, 2H), 7.71 (s, 2H), 7.24 (d, *J* = 3.9 Hz, 2H), 7.18 (s, 2H), 7.04 (s, 2H), 3.00 (d, *J* = 3.2 Hz, 4H), 2.94 – 2.66 (m, 8H), 1.71 (s, 8H), 1.54 – 1.16 (m, 42H), 1.03 – 0.78 (m, 24H). ¹³C NMR (125 MHz, CDCl₃) δ 146.00, 144.59, 142.55, 142.20, 141.22, 141.12, 138.11, 136.81, 135.88, 135.50, 130.69, 129.60, 129.11, 128.56, 125.87, 122.63, 119.42. IR (Neat): ν = 2956, 2923, 2855, (C=O) 1659, 1523, 1424, 1379, 1344, 1226, 1136, 1055, 848, 814, 671 cm⁻¹. MS(MALDI⁺) m/z calculated for C₇₆H₉₈O₂S₁₀[M+H⁺]: 1363.49, found: 1363.63. Elemental analysis calculated for C₇₆H₉₈O₂S₁₀: C, 66.91; H, 7.24; O, 2.35; S, 23.50. Found; C:66.74; H, 7.23; N: 0.00

S2.1.6 *Synthesis of 5'',5''''-(4,8-bis((triisopropylsilyl)ethynyl)benzo[1,2-b:4,5-b']dithiophene-2,6-diyl)bis(3',3''-dihexyl-[2,2':5',2''-terthiophene]-5-carbaldehyde) (16)*



Product formed a red powder. Yield = 0.74 g, (0.52 mmol, 74%). $R_f = 0.30$ (PS:DCM = 1:1) ^1H NMR (600 MHz, CDCl_3) δ 9.90 (s, 2H), 7.72 (d, $J = 3.9$ Hz, 2H), 7.61 (s, 2H), 7.26 (d, $J = 3.6$ Hz, 2H), 7.17 (s, 2H), 7.05 (s, 2H), 2.90 – 2.77 (m, 8H), 1.72 (t, $J = 7.7$ Hz, 8H), 1.49 – 1.19 (m, 66H), 0.95 – 0.86 (m, 12H). ^{13}C NMR (125 MHz, CDCl_3) δ 182.56, 145.99, 142.56, 142.26, 141.36, 140.15, 139.39, 138.20, 136.82, 135.77, 135.34, 130.82, 129.74, 129.36, 128.71, 125.97, 118.95, 111.24, 102.34, 102.20, 31.64, 30.41, 30.23, 29.75, 29.55, 29.21, 22.62, 22.59, 18.82, 14.09, 14.07, 11.35. IR (Neat): $\nu = 2940, 2863, 2196, 2065, 1460, 1375, 1203, 881, 657$ cm $^{-1}$. MS(MALDI $^+$) m/z calculated for $\text{C}_{82}\text{H}_{106}\text{O}_2\text{S}_8\text{Si}_2$ [M $^+$]: 1436.41, found: 1436.787. Elemental analysis calculated for $\text{C}_{82}\text{H}_{106}\text{O}_2\text{S}_8\text{Si}_2$: C, 68.57; H, 7.44; O, 2.23; S, 17.86; Si, 3.91. Found: C: 67.15; H, 7.24; N: 0.00

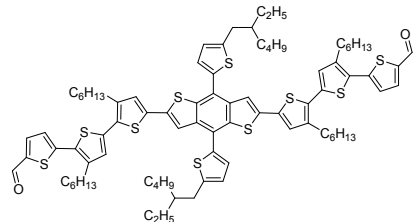
S2.1.7 *Synthesis of 5'',5''''-(4,8-bis(5-hexylthiophen-2-yl)benzo[1,2-b:4,5-b']dithiophene-2,6-diyl)bis(3',3''-dihexyl-[2,2':5',2''-terthiophene]-5-carbaldehyde) (17)*



Product formed a red powder. Yield = 0.78 g (0.56 mmol, 86%). $R_f = 0.25$ (PS:DCM = 1:1) ^1H NMR (400 MHz, CDCl_3) δ 9.88 (s, 2H), 7.70 (d, $J = 3.9$ Hz, 2H), 7.61 (s, 2H), 7.31 (d, $J = 3.5$ Hz, 2H), 7.22 (d, $J = 3.9$ Hz, 2H), 7.11 (s, 2H), 7.01 (s, 2H), 6.96 (d, $J = 3.4$ Hz, 2H), 2.96 (t, J

δ = 7.7 Hz, 4H), 2.84 – 2.78 (m, 4H), 2.77 – 2.72 (m, 4H), 1.86 – 1.80 (m, 4H), 1.72 – 1.64 (m, 8H), 1.53 – 1.47 (m, 4H), 1.46 – 1.29 (m, 32H), 0.97 – 0.88 (m, 18H). ^{13}C NMR (125 MHz), CDCl_3) δ 182.50, 147.43, 146.02, 142.52, 142.16, 141.13, 138.72, 137.44, 137.36, 136.79, 136.48, 135.95, 135.51, 130.33, 129.47, 129.03, 128.39, 127.89, 125.82, 124.38, 123.37, 119.13, 31.62, 31.59, 31.51, 30.33, 30.30, 30.19, 29.76, 29.63, 29.24, 29.22, 28.96, 22.61, 22.57, 14.10, 14.06, 14.04. IR (Neat): ν = 2954, 2924, 2855, 1741, (C=O) 1661, 1454, 1377, 1223, 1057, 1019, 802, 670 cm^{-1} . MS(MALDI $^+$) m/z calculated for $\text{C}_{80}\text{H}_{94}\text{O}_2\text{S}_{10}$ [M+H $^+$]: 1407.46, found: 1407.693. Elemental analysis calculated for $\text{C}_{80}\text{H}_{94}\text{O}_2\text{S}_{10}$: C, 68.23; H, 6.73; O, 2.27; S, 22.77. Found: C: 68.15; H, 6.72; N: 0.00

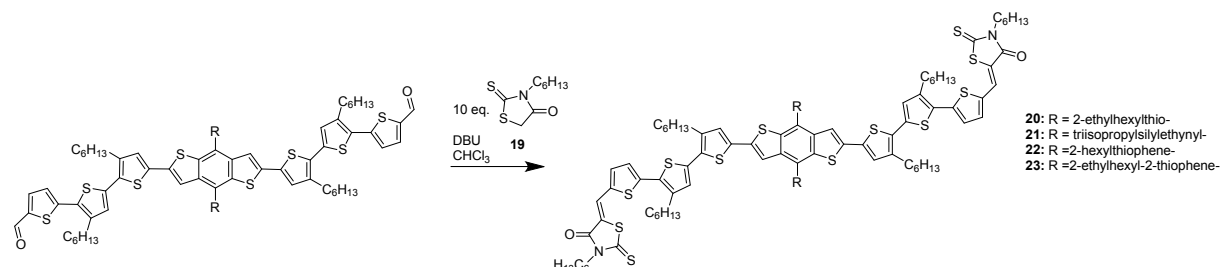
S2.1.8 Synthesis of 5'',5''''-(4,8-bis(5-(2-ethylhexyl)thiophen-2-yl)benzo[1,2-b:4,5-b']dithiophene-2,6-diyl)bis(3',3''-dihexyl-[2,2':5',2''-terthiophene]-5-carbaldehyde) (18)



Product formed a red powder. Yield = 0.78 g (0.54 mmol, 89%). ^1H NMR (600 MHz, CDCl_3) δ 9.89 (s, 2H), 7.71 (d, J = 3.9 Hz, 2H), 7.63 (s, 2H), 7.31 (d, J = 3.5 Hz, 2H), 7.23 (d, J = 4.0 Hz, 2H), 7.12 (s, 2H), 7.02 (s, 2H), 6.94 (d, J = 3.5 Hz, 2H), 2.90 (dd, J = 6.9, 3.7 Hz, 2H), 2.79 (dt, J = 20.8, 7.9 Hz, 8H), 1.77 – 1.63 (m, 8H), 1.53 – 1.23 (m, 44H), 1.05 – 0.81 (m, 24H). ^{13}C NMR (125 MHz, CDCl_3) δ 182.52, 146.07, 146.03, 142.52, 142.19, 141.17, 138.71, 137.44, 137.35, 136.80, 136.70, 135.94, 135.56, 130.34, 129.49, 129.07, 128.38, 127.79, 125.86, 125.47, 123.40, 119.20, 41.47, 34.34, 32.49, 31.62, 31.60, 30.35, 30.19, 29.75, 29.61, 29.22, 29.21, 28.93, 25.83, 23.03, 22.56, 14.18, 14.05, 14.04, 10.96. IR (Neat): ν = 2955, 2922, 2853, 1741, (C=O) 1657, 1454, 1377, 1223, 1051, 1019, 800, 671 cm^{-1} . MS(MALDI $^+$) m/z calculated

for $C_{84}H_{102}O_2S_{10}$ $[M^+]$: 1463.51, found: 1463.08. Elemental analysis calculated for $C_{84}H_{102}O_2S_{10}$: C, 68.90; H, 7.02; O, 2.19; S, 21.90. Found: C:70.08; H, 6.91; N: 0.00

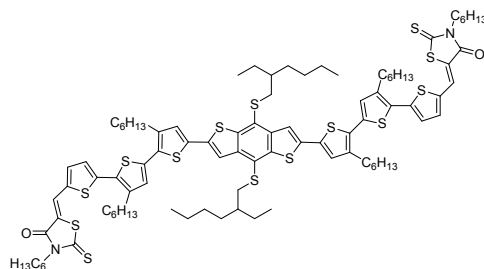
S2.2 General synthesis of BTR Analogue Molecules



General procedure for the Knovenagel condensation

The corresponding BTR-dialdehyde core (200 mg) and n-hexyl rhodanine (10 eq.) were dissolved in chloroform (5 mL). Catalytic DBU (5 drops) was added to this solution, which was then stirred for 2 hours. The solvent was then removed under reduced pressure, and the crude mixture purified via column chromatography (silica, 1:1 petroleum spirits: chloroform unless otherwise noted) and size-exclusion chromatography (toluene, Biobeads) and precipitated in methanol to yield the product.

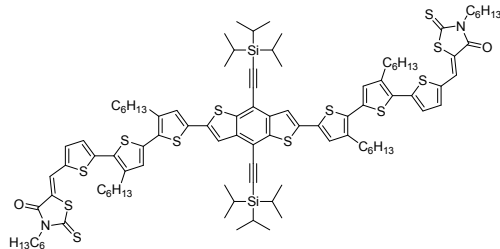
S2.2.1 (*5Z,5'Z*)-5,5'-((5'',5''''-(4,8-bis((2-ethylhexyl)thio)benzo[1,2-*b*:4,5-*b*']dithiophene-2,6-diyl)bis(3',3''-dihexyl-[2,2':5',2''-terthiophene]-5'',5-diyl))bis(methanylylidene))bis(3-hexyl-2-thioxothiazolidin-4-one) (**20**, BTR-TE)



Product formed a purple powder. Yield = 0.21 g (0.12 mmol, 82%). $R_f = 0.80$ (PS:CHCl₃ = 1:1)¹H NMR (400 MHz, CDCl₃) δ 7.81 (s, 2H), 7.65 (d, J = 1.8 Hz, 2H), 7.34 (d, J = 3.9 Hz, 2H), 7.20 (d, J = 3.9 Hz, 2H), 7.15 (s, 2H), 7.01 (s, 2H), 4.19 – 4.01 (t, 4H), 2.99 (d, J = 3.6 Hz, 4H), 2.81 (dt, J = 16.8, 8.0 Hz, 10H), 1.72 (ddd, J = 9.5, 7.5, 3.7 Hz, 14H), 1.60 – 1.18 (m,

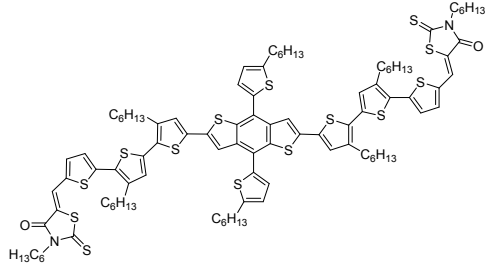
52H), 1.03 – 0.80 (m, 30H). ^{13}C NMR (125 MHz, CDCl_3) δ 192.10, 167.43, 144.53, 144.24, 141.88, 141.07, 140.98, 138.01, 137.00, 135.53, 135.33, 134.58, 130.84, 129.75, 128.97, 128.49, 126.40, 124.89, 122.50, 120.15, 119.31. IR (Neat): ν = 2955, 2923, 2856, 1698, 1578, 1424, 1181, 820 cm^{-1} . MS(MALDI) m/z calculated for $\text{C}_{94}\text{H}_{124}\text{N}_2\text{O}_2\text{S}_{14}$ [M+H $^+$]: 1762.56, found: 1762.34. Elemental analysis calculated for $\text{C}_{94}\text{H}_{124}\text{N}_2\text{O}_2\text{S}_{14}$: C, 64.04; H, 7.09; N, 1.59; O, 1.82; S, 25.46. Found: C, 64.10; H, 7.12; N, 1.48; S, 25.17

S2.2.2 (*5Z,5'Z*)-5,5'-((5'',5''''-(4,8-bis((triisopropylsilyl)ethynyl)benzo[1,2-*b*:4,5-*b'*]dithiophene-2,6-diyl)bis(3',3''-dihexyl-[2,2':5',2''-terthiophene]-5'',5-diyl))bis(methanylylidene))bis(3-hexyl-2-thioxothiazolidin-4-one) (21, BTR-TIPS)



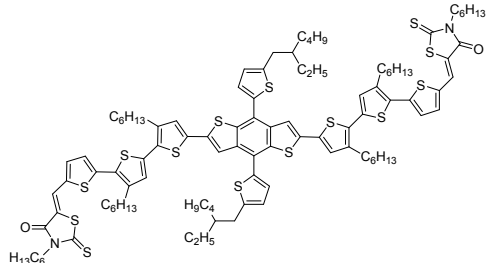
Product formed a purple powder. Yield = 0.20 g (0.11nmol, 79%). R_f = 0.80 (PS: CHCl_3 = 3:2) ^1H NMR (400 MHz, CDCl_3) δ 7.81 (s, 2H), 7.50 (s, 2H), 7.34 (s, 2H), 7.21 (s, 2H), 7.08 (s, 2H), 6.98 (s, 2H), 4.05 (dd, J = 8.8, 6.8 Hz, 4H), 2.81 (dt, J = 19.0, 7.9 Hz, 8H), 1.71 (dt, J = 12.2, 5.8 Hz, 12H), 1.53 – 1.19 (m, 778H), 0.99 – 0.90 (m, 12H), 0.93 – 0.85 (m, 6H). ^{13}C NMR (125 MHz, CDCl_3) δ 192.11, 167.42, 144.18, 141.83, 140.98, 140.02, 139.35, 138.11, 137.00, 135.30, 135.03, 134.56, 131.03, 129.83, 129.13, 128.58, 126.42, 124.95, 120.06, 118.72, 111.05, 102.34, 102.17. IR (Neat): ν = 2940, 2889, 2863, 2196, 2065, 1460, 1375, 1203, 881, 657 cm^{-1} . MS(MALDI) m/z calculated for $\text{C}_{100}\text{H}_{132}\text{N}_2\text{O}_2\text{S}_{12}\text{Si}_2$ [M+H $^+$]: 1834.66, found: 1834.45. Elemental analysis calculated for $\text{C}_{100}\text{H}_{132}\text{N}_2\text{O}_2\text{S}_{12}\text{Si}_2$: C, 65.45; H, 7.25; N, 1.53; O, 1.74; S, 20.97; Si, 3.06. Found: C, 65.46; H, 7.32; N, 1.47; S, 21.04

S2.2.3 (*5Z,5'Z*)-5,5'-((5'',5''''-(4,8-bis(5-hexylthiophen-2-yl)benzo[1,2-*b*:4,5-*b*']dithiophene-2,6-diyl)bis(3',3''-dihexyl-[2,2':5',2''-terthiophene]-5'',5-diyl))bis(methanylylidene))bis(3-hexyl-2-thioxothiazolidin-4-one) (**22, BTR-H**)



Product formed a purple powder. Yield =0.18 g (0.10 mmol, 70%). $R_f = 0.75$ (PS:CHCl₃ = 2:1)¹H NMR (400 MHz, CDCl₃) 7.82 (s, 2H), 7.58 (s, 2H), 7.34 (d, *J* = 3.9 Hz, 2H), 7.31 (d, *J* = 3.8 Hz, 2H), 7.19 (d, *J* = 4.9 Hz, 2H), 7.09 (s, 2H), 6.99 (s, 2H), 6.96 (d, *J* = 2.6 Hz, 2H), 4.14 – 4.05 (m, 4H), 2.97 (t, *J* = 7.8 Hz, 4H), 2.81 (t, *J* = 7.9 Hz, 4H), 2.75 (t, *J* = 8.0 Hz, 4H), 1.94 – 1.79 (m, 4H), 1.80 – 1.64 (m, 12H), 1.53 – 1.22 (m, 48H), 1.02 – 0.80 (m, 24H).¹³C NMR (125 MHz, CDCl₃) δ 147.40, 144.24, 141.90, 140.99, 138.68, 137.42, 137.34, 137.04, 136.51, 135.61, 135.40, 134.61, 130.47, 129.66, 129.02, 128.38, 127.90, 126.49, 124.94, 124.38, 123.31, 120.20, 119.08. IR (Neat): ν = 2954, 2924, 2853, 1699, 1578, 1424, 1184, 1066, 802, 670 cm⁻¹. MS(MALDI) m/z calculated for C₉₈H₁₂₀N₂O₂S₁₄ [M+H⁺]:1806.56, found: 1806.28 . Elemental analysis calculated for C₉₈H₁₂₀N₂O₂S₁₄: C, 65.14; H, 6.69; N, 1.55; O, 1.77; S, 24.84. Found: C, 64.57; H, 6.66; N, 1.85; S, 25.34

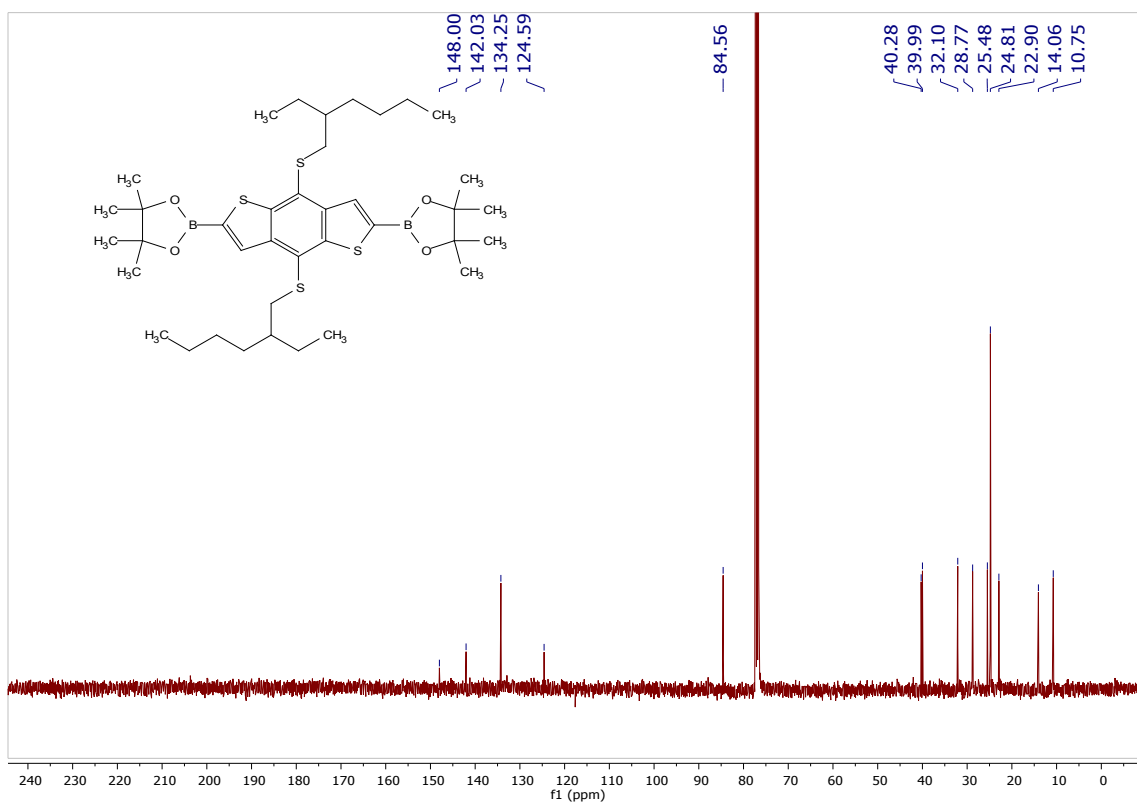
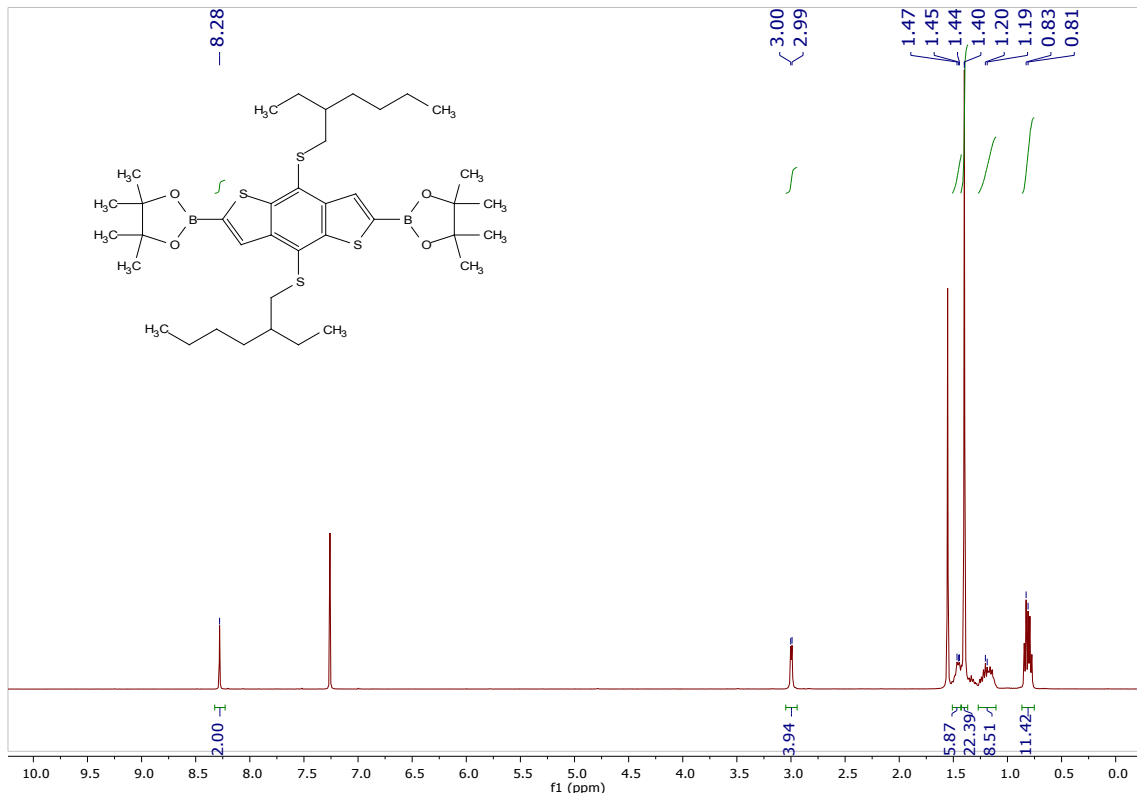
(5Z,5'Z)-5,5'-((5'',5''''-(4,8-bis(5-(2-ethylhexyl)thiophen-2-yl)benzo[1,2-b:4,5-b']dithiophene-2,6-diyl)bis(3',3''-dihexyl-[2,2':5',2''-terthiophene]-5'',5-diyl))bis(methanylylidene))bis(3-hexyl-2-thioxothiazolidin-4-one) (23, BTR-EH)



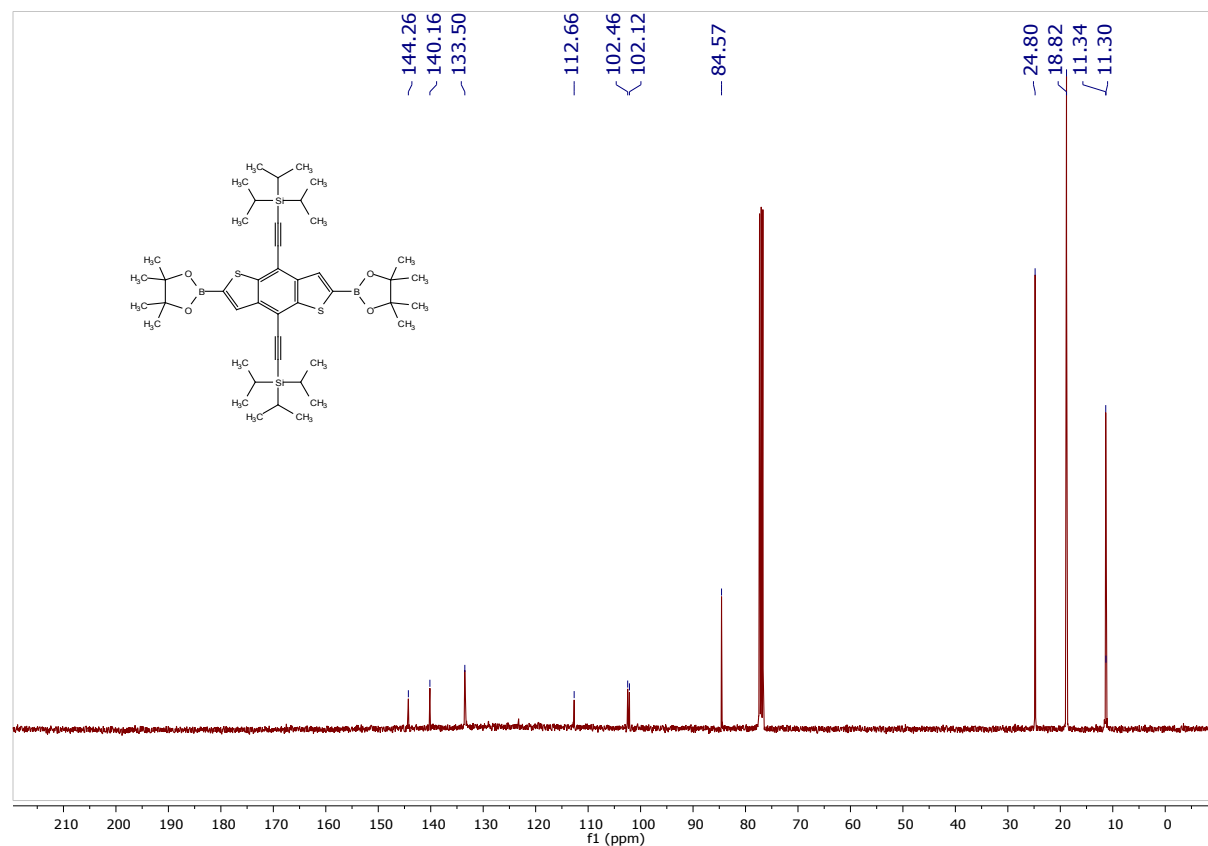
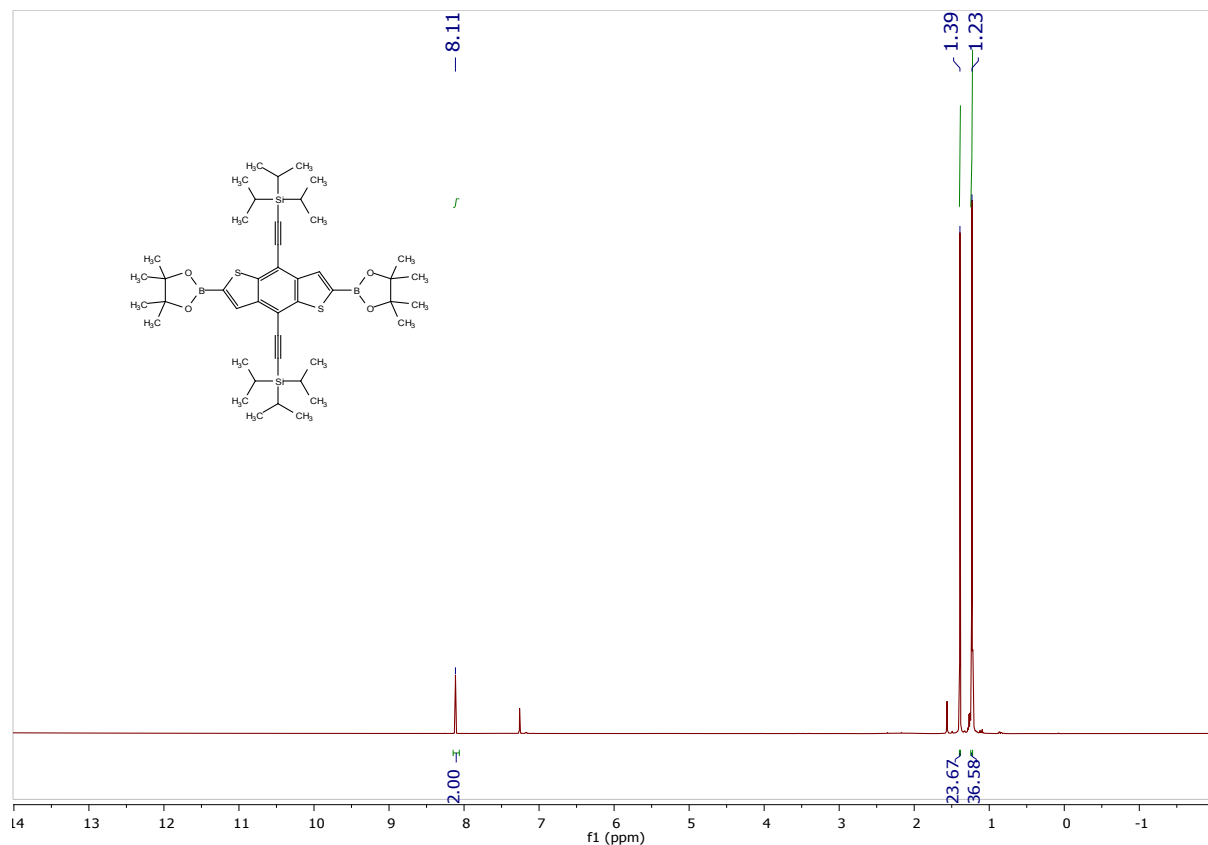
Product formed a purple powder. Yield = 0.16 g (0.09 mmol, 68%). R_f = 0.75 (PS:DCM = 1:1)¹H NMR (400 MHz, CDCl₃) δ 7.83 (s, 2H), 7.60 (s, 2H), 7.35 (d, *J* = 4.0 Hz, 2H), 7.32 (d, *J* = 3.4 Hz, 2H), 7.19 (d, *J* = 4.0 Hz, 2H), 7.09 (s, 2H), 6.99 (s, 2H), 6.94 (d, *J* = 3.4 Hz, 2H), 4.13 – 4.05 (m, 4H), 2.91 (t, *J* = 6.6 Hz, 4H), 2.78 (dt, *J* = 30.0, 8.0 Hz, 4H), 1.74 – 1.64 (m, 16H), 1.52 – 1.29 (m, 54H), 1.02 – 0.86 (m, 30H). ¹³C NMR (125 MHz, CDCl₃) δ 192.11, 167.44, 145.97, 144.24, 141.86, 140.94, 138.62, 137.35, 137.29, 136.99, 136.77, 135.60, 135.39, 134.58, 130.47, 129.64, 128.95, 128.31, 127.80, 126.42, 125.45, 124.91, 123.26, 120.14, 119.09, 44.83, 41.48, 34.36, 32.51, 31.68, 31.64, 31.30, 30.28, 30.25, 29.84, 29.69, 29.67, 29.30, 29.27, 29.24, 28.95, 26.90, 26.42, 25.84, 23.06, 22.64, 22.60, 22.48, 14.21, 14.10, 13.97, 10.98. IR (Neat): ν = 2956, 2921, 2851, 1699, 1579, 1424, 1184, 1066, 802, 670 cm⁻¹. MS(MALDI) m/z calculated for C₁₀₂H₁₂₈N₂O₂S₁₄[M+H⁺]: 1862.62, found: 1862.45. Elemental analysis calculated for C₁₀₂H₁₂₈N₂O₂S₁₄: C, 65.76; H, 6.93; N, 1.50; O, 1.72; S, 24.10. Found: C, 65.72; H, 6.85; N, 1.62; S, 23.98

S3 ^1H and ^{13}C NMR Spectra

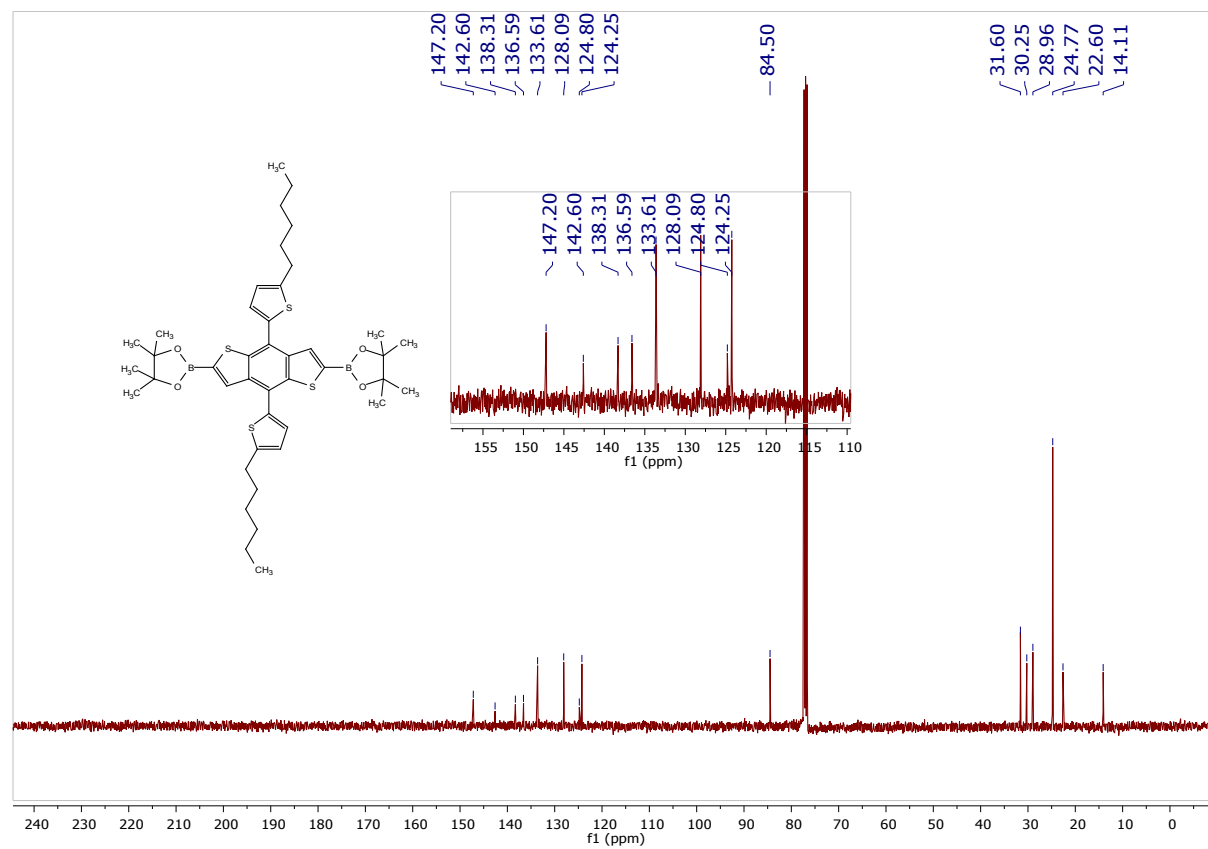
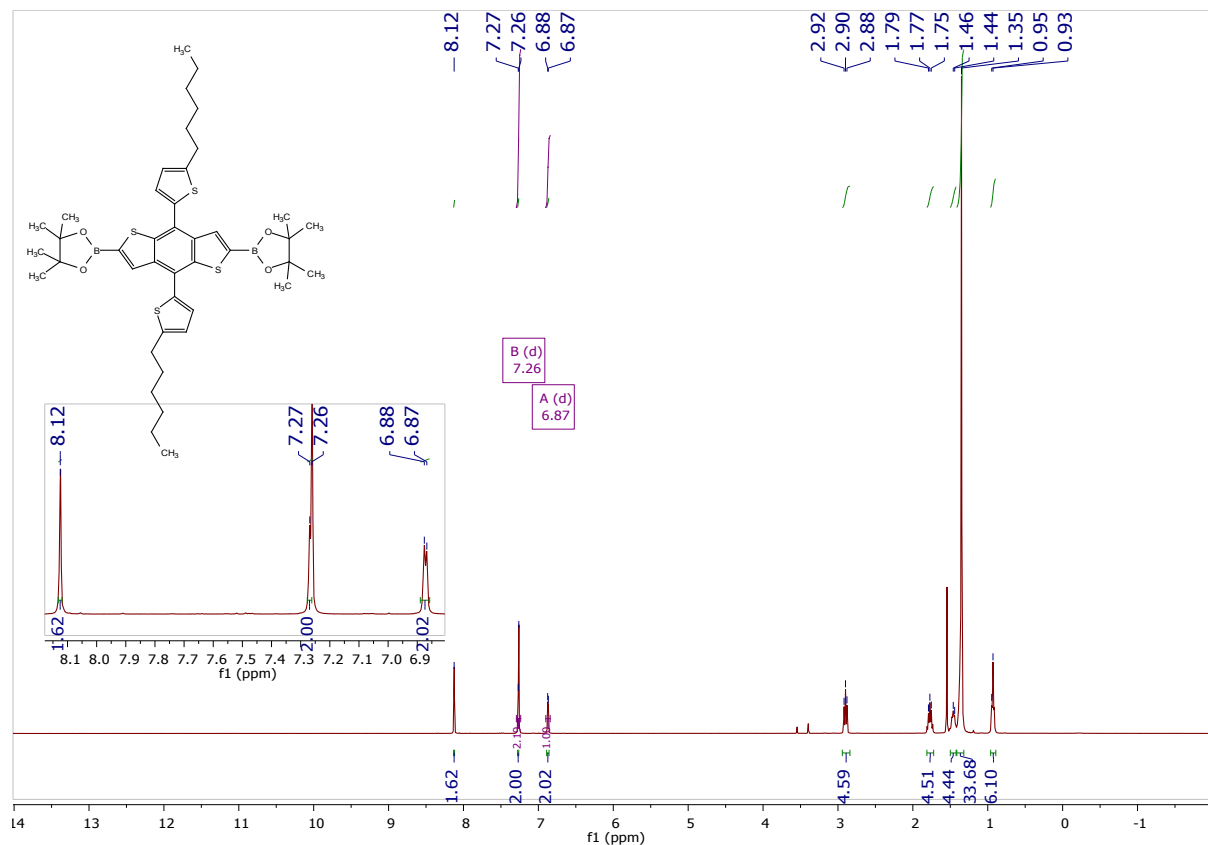
*S3.1 2,2'-(4,8-bis((2-ethylhexyl)thio)benzo[1,2-*b*:4,5-*b'*]dithiophene-2,6-diyl)bis(4,4,5,5-tetramethyl-1,3,2-dioxaborolane) (10)*



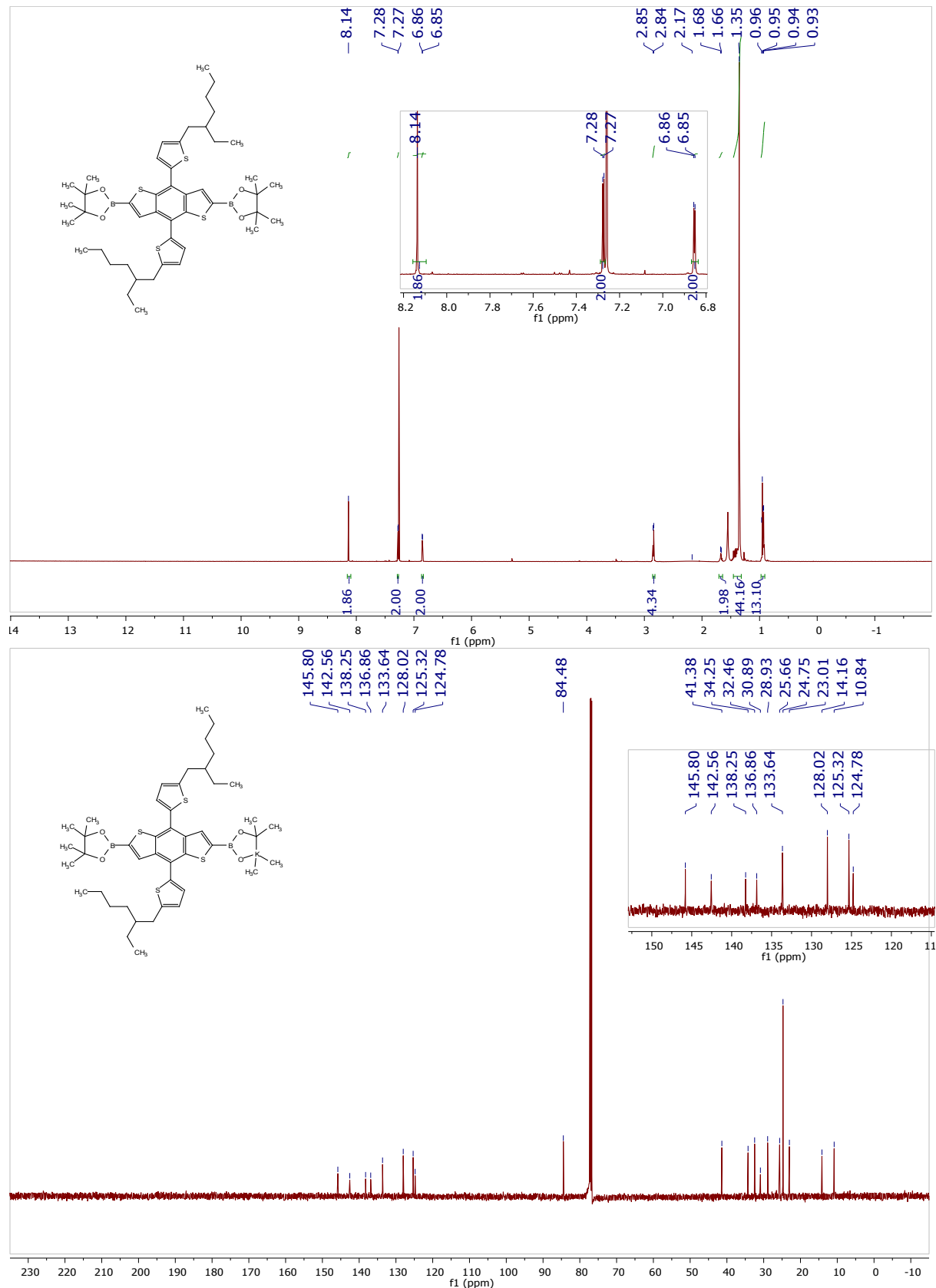
*S3.2 ((2,6-bis(4,4,5,5-tetramethyl-1,3,2-dioxaborolan-2-yl)benzo[1,2-*b*:4,5-*b*']dithiophene-4,8-diyl)bis(ethyne-2,1-diyl))bis(triisopropylsilane) (11)*



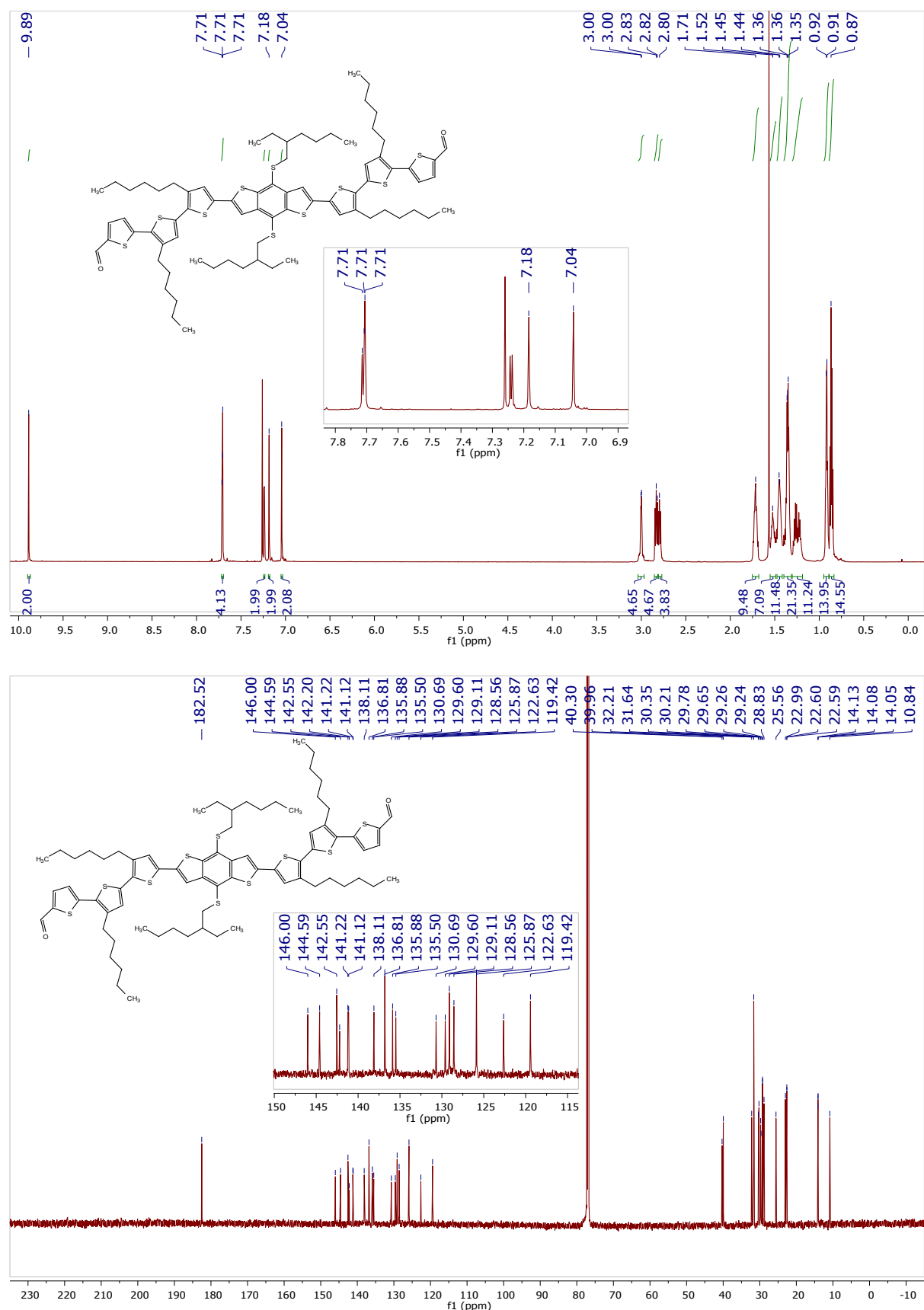
*S3.3 2,2'-(4,8-bis(5-hexylthiophen-2-yl)benzo[1,2-*b*:4,5-*b'*]dithiophene-2,6-diyl)bis(4,4,5,5-tetramethyl-1,3,2-dioxaborolane) (12)*



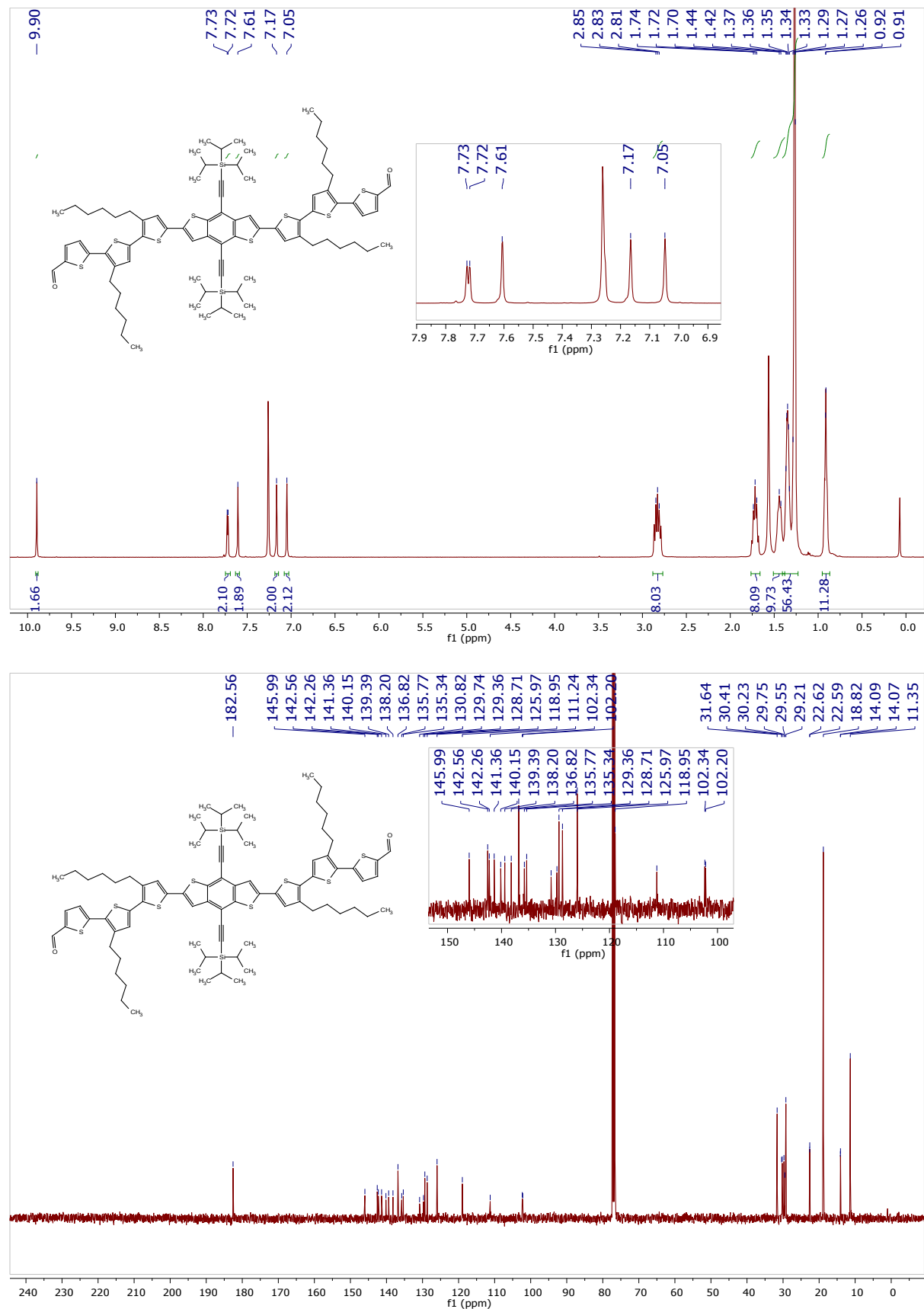
*S3.4 2,2'-(4,8-bis(5-(2-ethylhexyl)thiophen-2-yl)benzo[1,2-*b*:4,5-*b*']dithiophene-2,6-diyl)bis(4,4,5,5-tetramethyl-1,3,2-dioxaborolane) (13)*



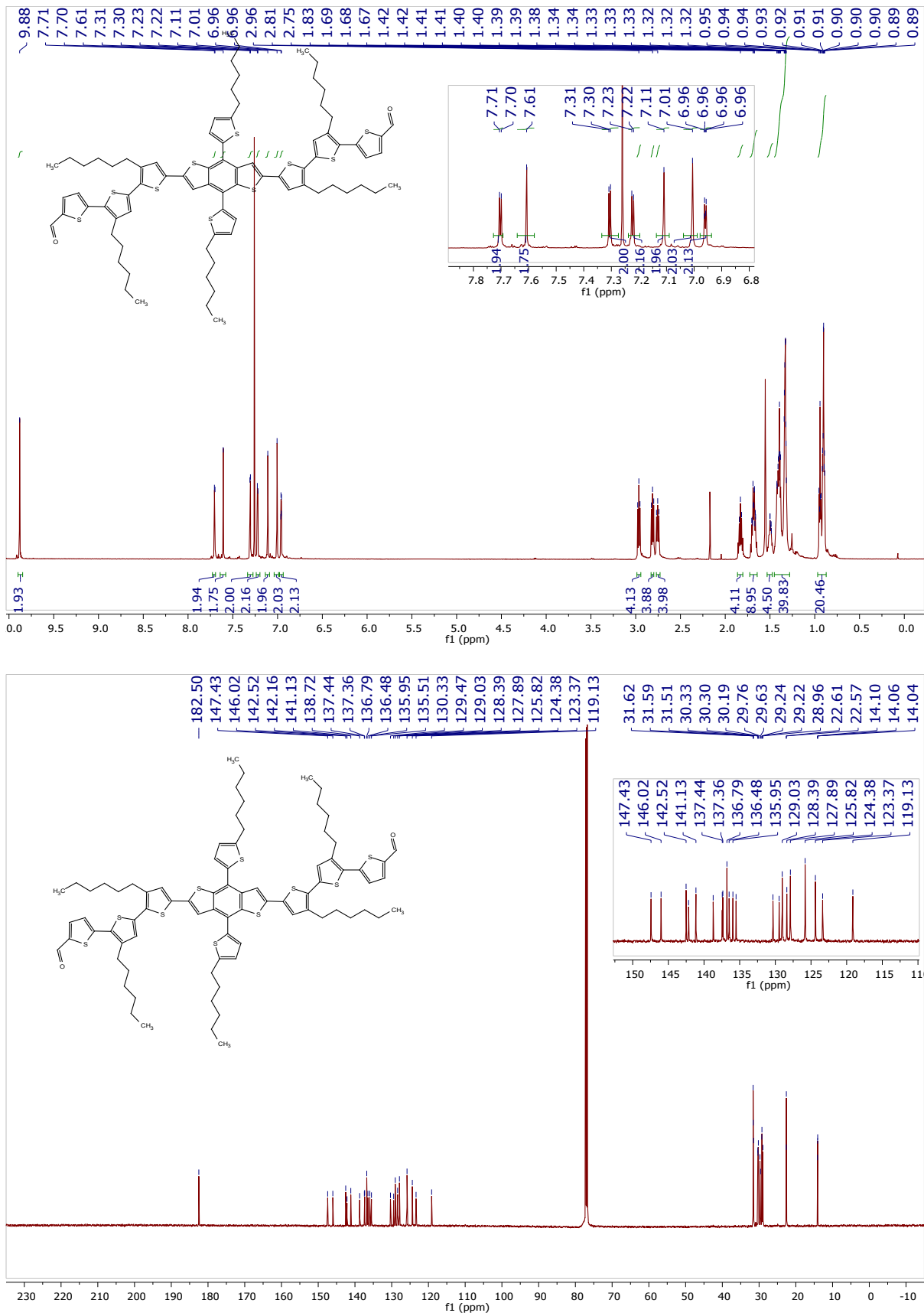
S3.5 5'',5''''-(4,8-bis((2-ethylhexyl)thio)benzo[1,2-*b*:4,5-*b*']dithiophene-2,6-diyl)bis(3',3''-dihexyl-[2,2':5',2''-terthiophene]-5-carbaldehyde) (**15**)



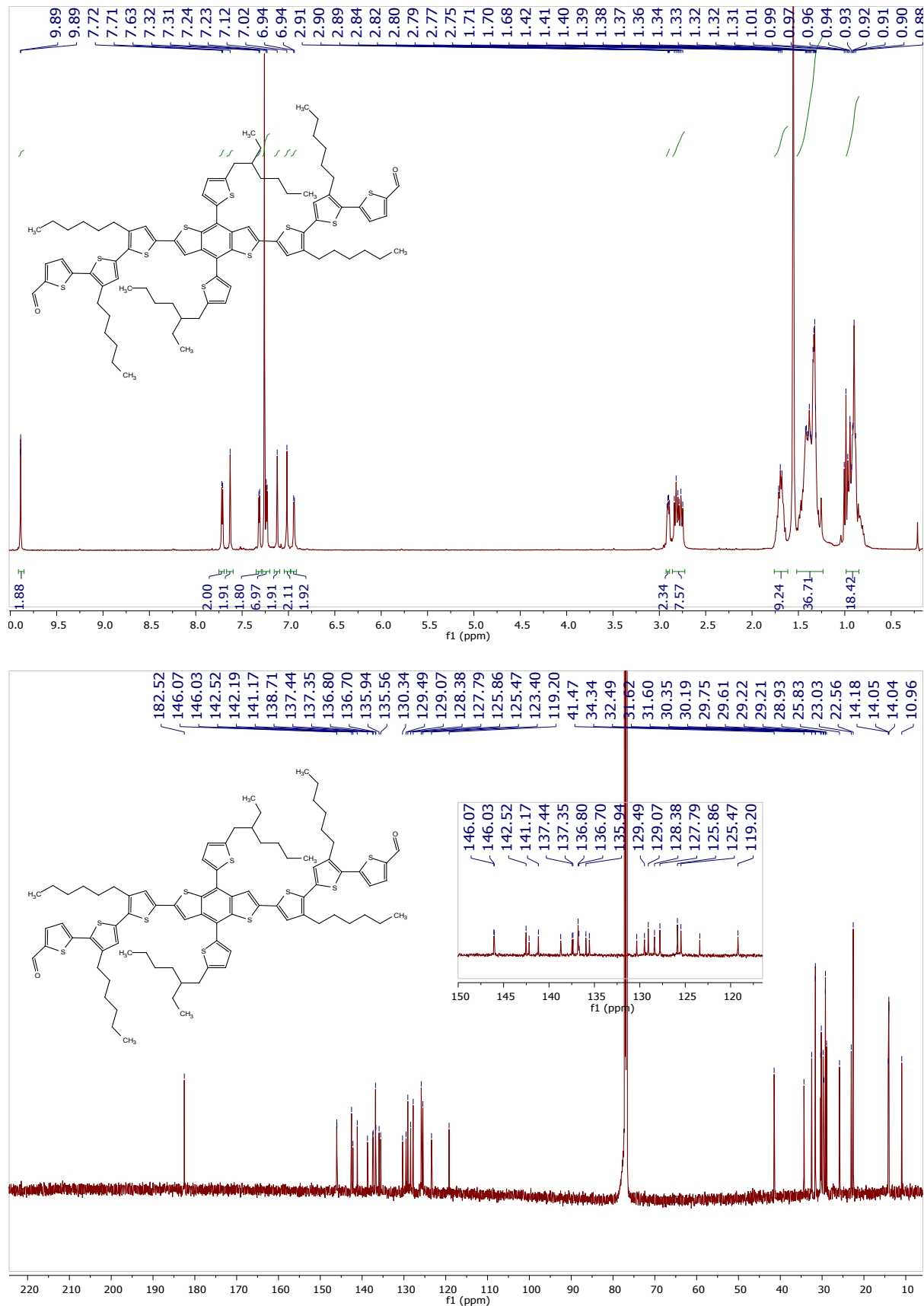
*S3.6 5'',5''''-(4,8-bis((triisopropylsilyl)ethynyl)benzo[1,2-*b*:4,5-*b'*]dithiophene-2,6-diyl)bis(3',3''-dihexyl-[2,2':5',2''-terthiophene]-5-carbaldehyde) (16)*



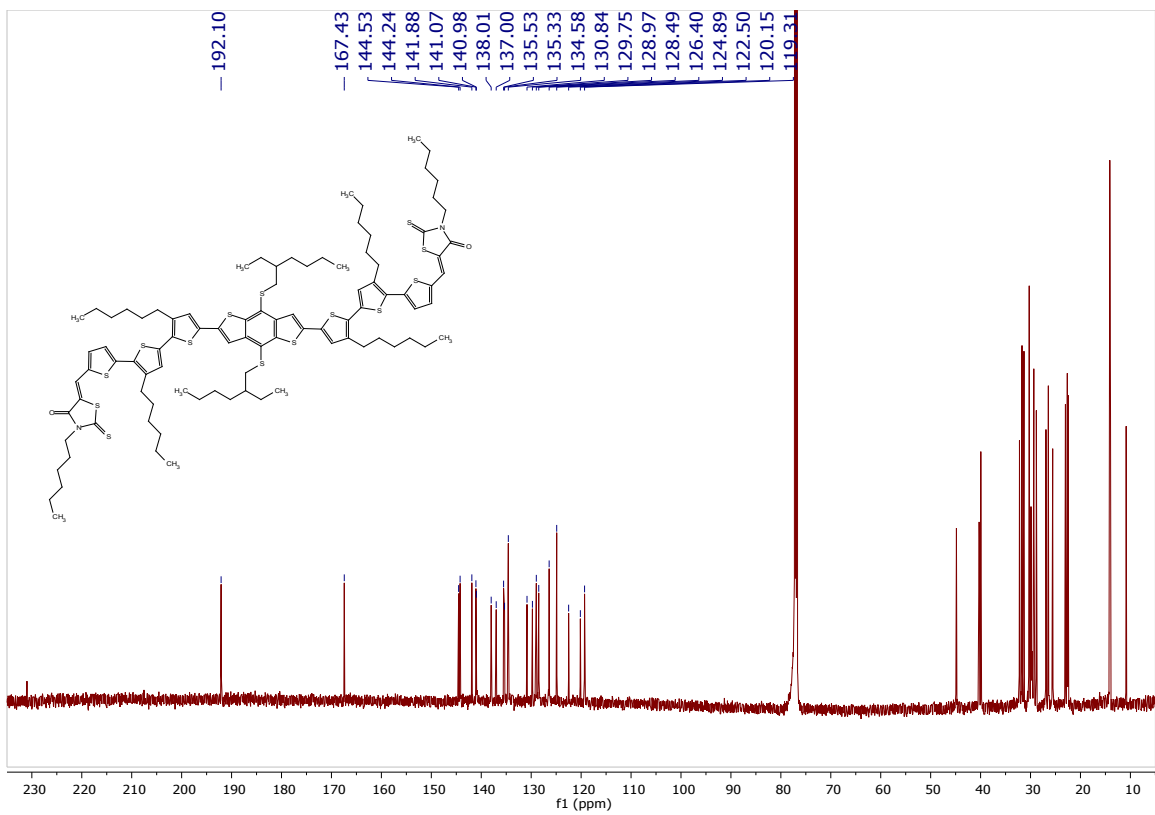
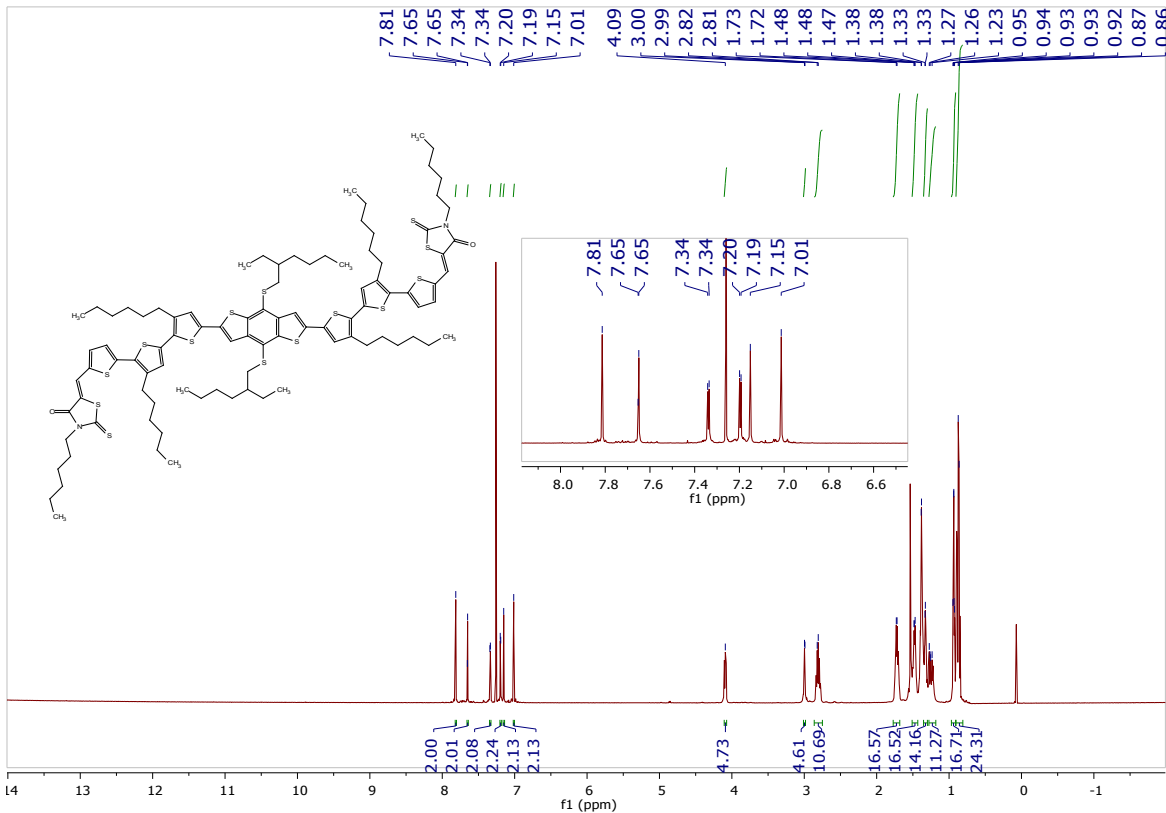
S3.7 5",5"""-*(4,8-bis(5-hexylthiophen-2-yl)benzo[1,2-*b*:4,5-*b'*]dithiophene-2,6-diyl)bis(3',3"-dihexyl-[2,2':5',2"-terthiophene]-5-carbaldehyde*) (**17**)



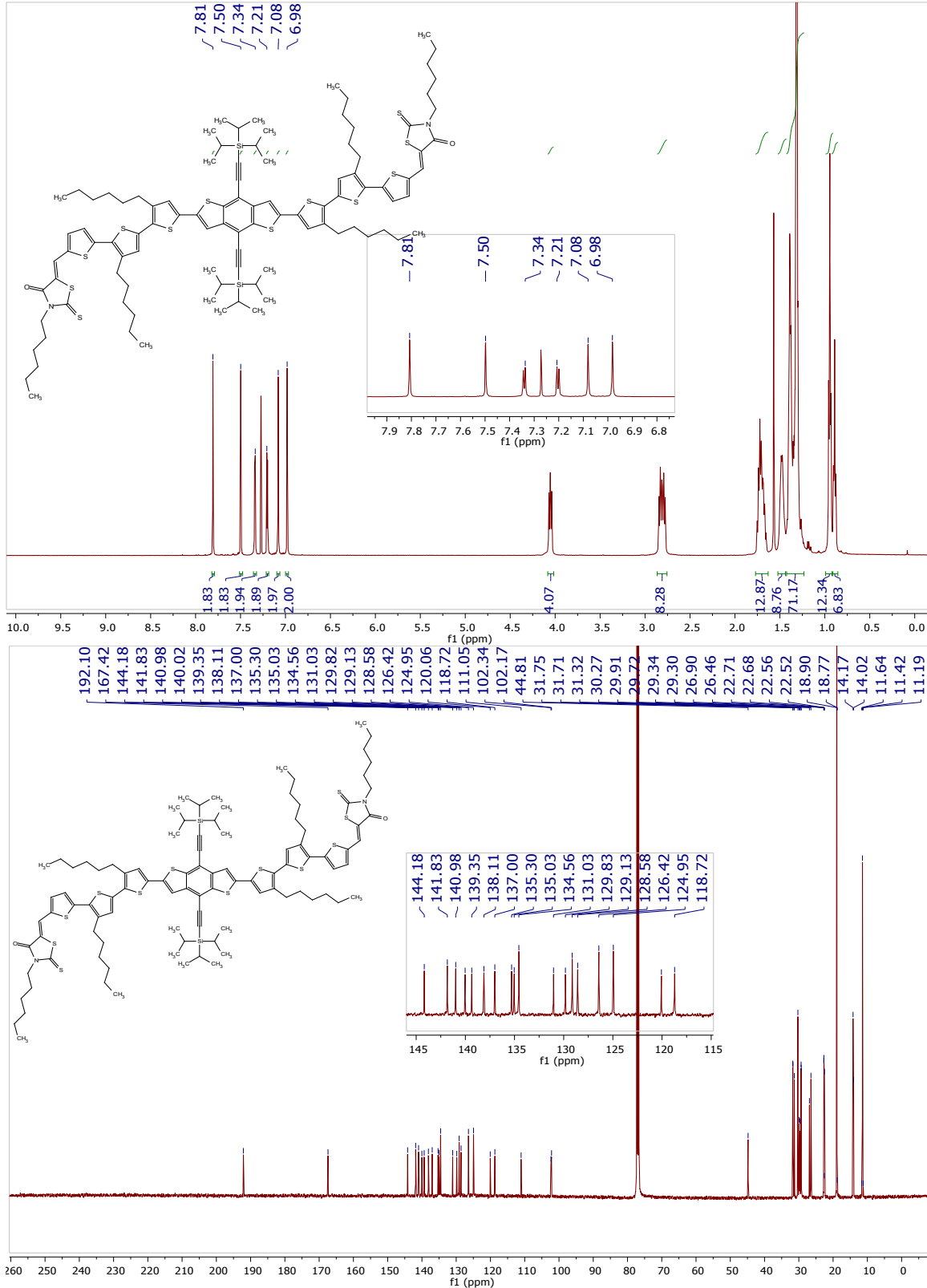
S3.8 5",5"""-*(4,8-bis(5-(2-ethylhexyl)thiophen-2-yl)benzo[1,2-*b*:4,5-*b*']dithiophene-2,6-diyl)bis(3',3"-dihexyl-[2,2':5',2"-terthiophene]-5-carbaldehyde*) (18)



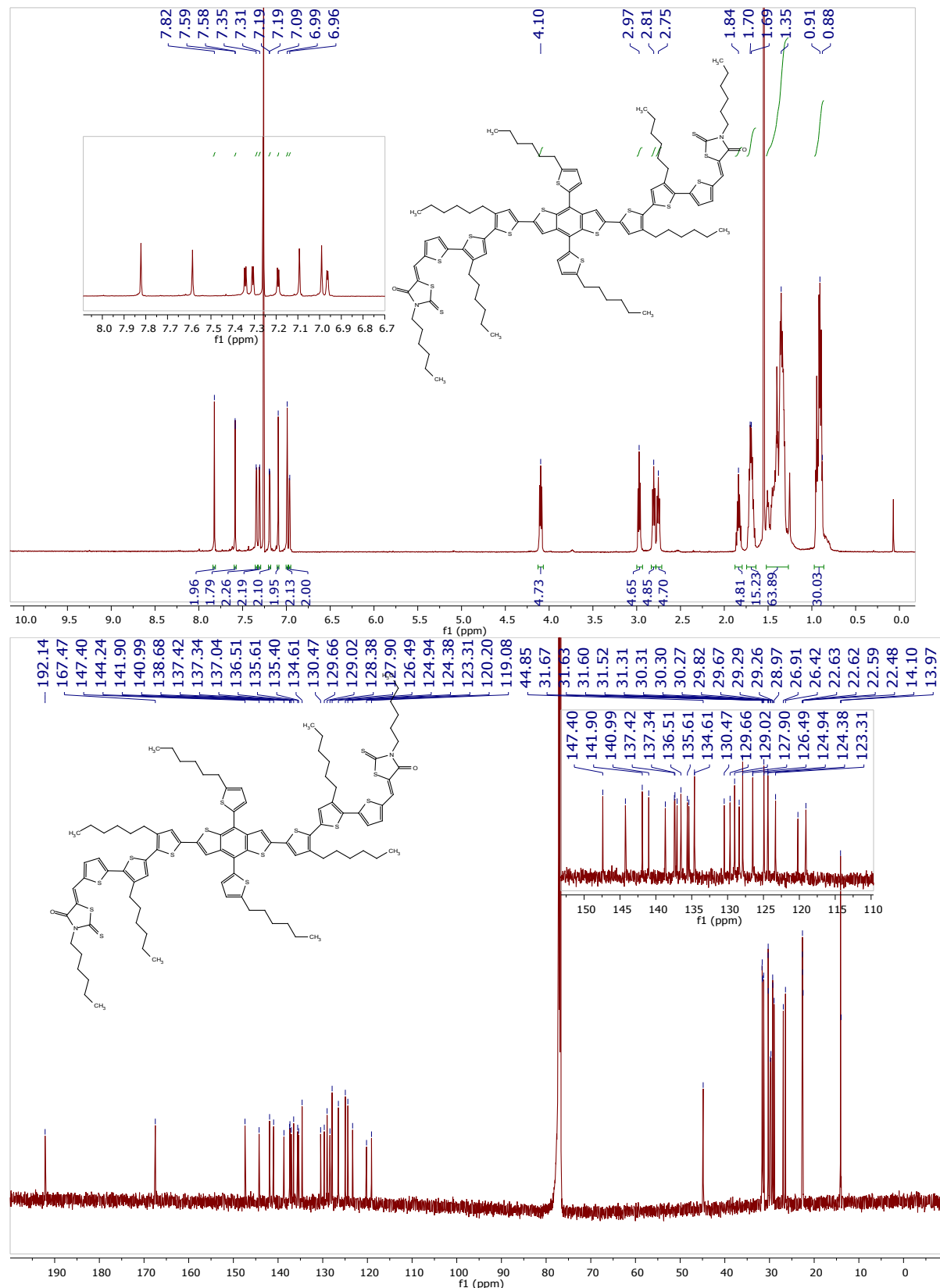
S3.9 (*5Z,5'Z*)-5,5'-((5'',5''''-(4,8-bis((2-ethylhexyl)thio)benzo[1,2-*b*:4,5-*b*']dithiophene-2,6-diyl)bis(3',3''-dihexyl-[2,2':5',2''-terthiophene]-5'',5-diyl))bis(methanylylidene))bis(3-hexyl-2-thioxothiazolidin-4-one) (**BTR-TE**)



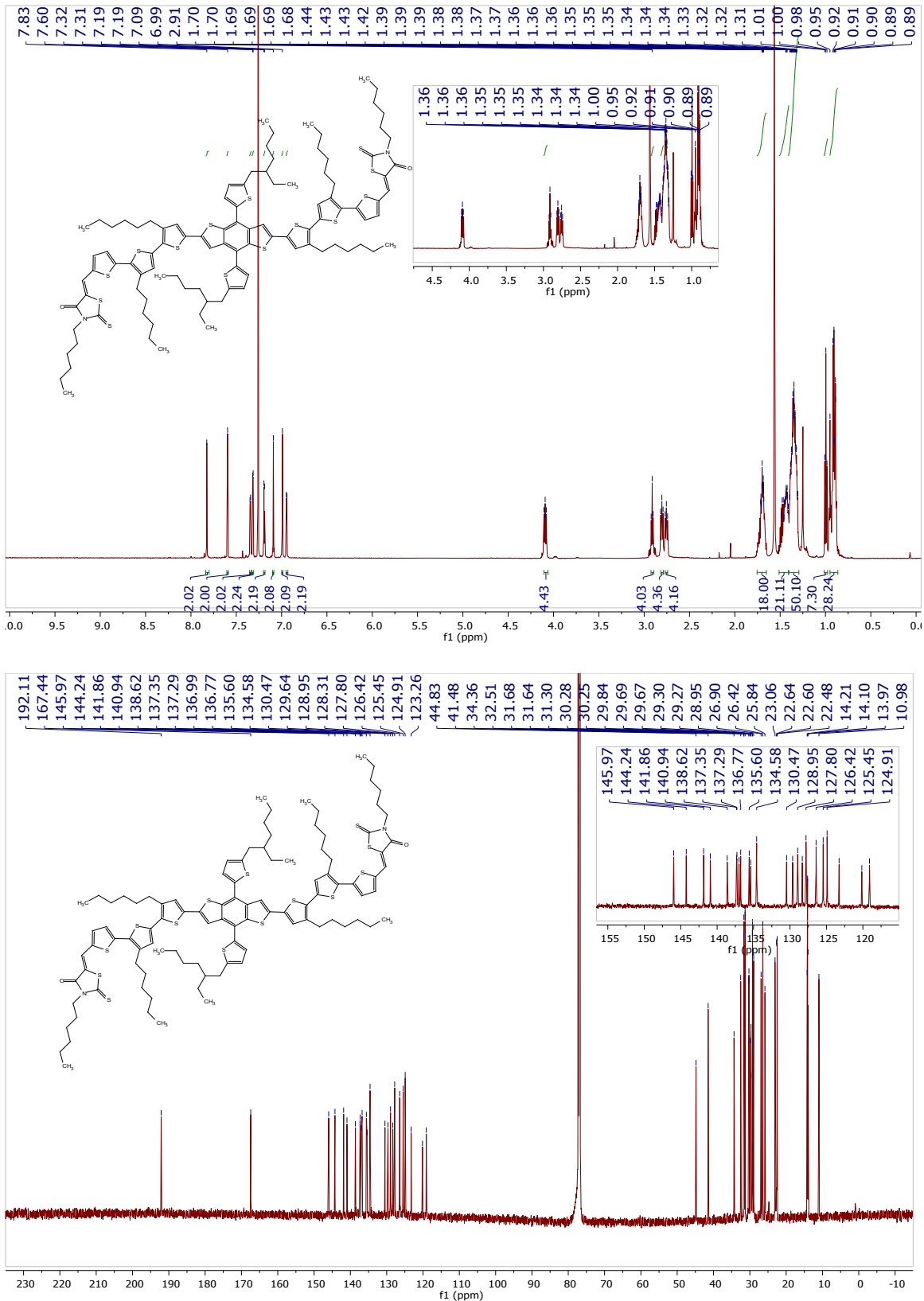
S3.10 (5Z,5'Z)-5,5'-((5'',5''''-(4,8-bis((triisopropylsilyl)ethynyl)benzo[1,2-b:4,5-b']dithiophene-2,6-diyl)bis(3',3''-dihexyl-[2,2':5',2''-terthiophene]-5'',5-diyl))bis(methanylylidene))bis(3-hexyl-2-thioxothiazolidin-4-one) (**BTR-TIPS**)



S3.11 (5Z,5'Z)-5,5'-((5'',5''''-(4,8-bis(5-hexylthiophen-2-yl)benzo[1,2-b:4,5-b']dithiophene-2,6-diyl)bis(3',3''-dihexyl-[2,2':5',2''-terthiophene]-5'',5-diyl))bis(methanylylidene))bis(3-hexyl-2-thioxothiazolidin-4-one) (BTR-H)

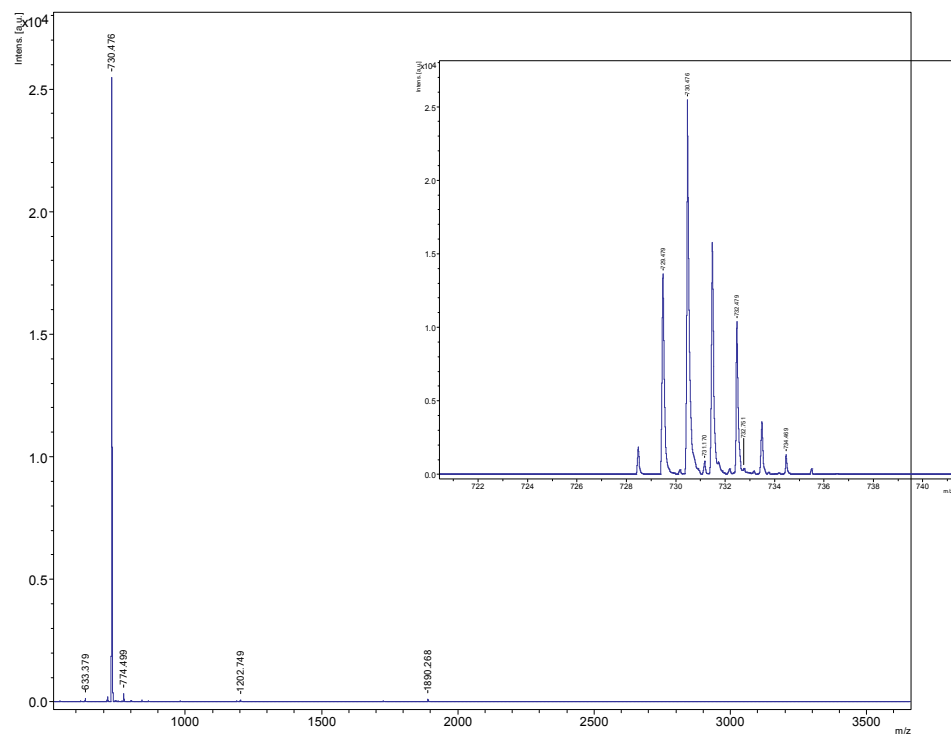


S3.12 (*5Z,5'Z*)-5,5'-((5'',5''''-(4,8-bis(5-(2-ethylhexyl)thiophen-2-yl)benzo[1,2-*b*:4,5-*b*]dithiophene-2,6-diyl)bis(3',3''-dihexyl-[2,2':5',2''-terthiophene]-5'',5-diyl))bis(methanylylidene))bis(3-hexyl-2-thioxothiazolidin-4-one) (**BTR-EH**)

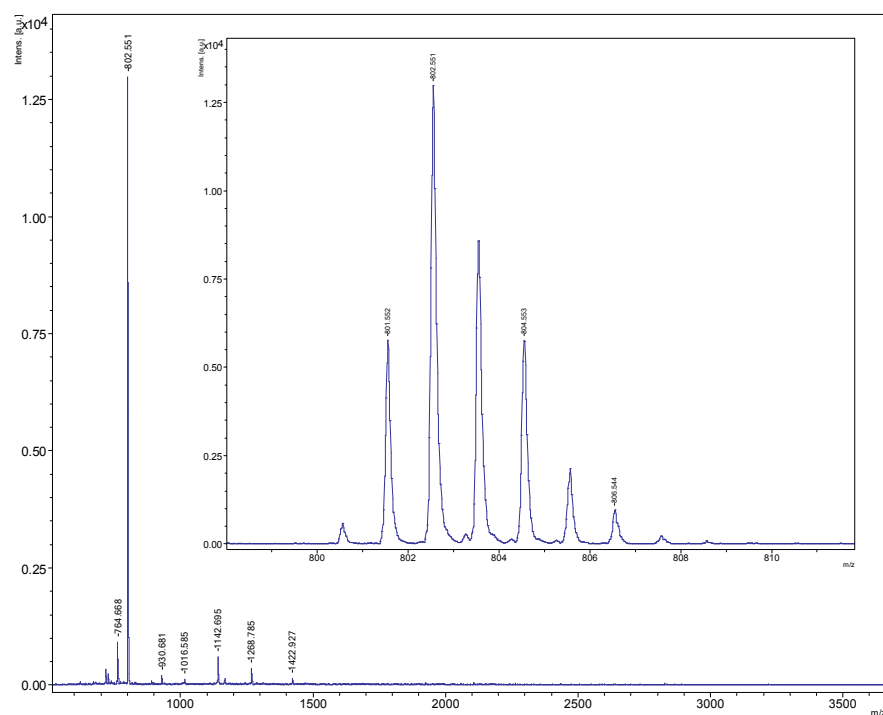


S4 MALDI spectra for the BTR-dialdehyde and BTR-analogue materials

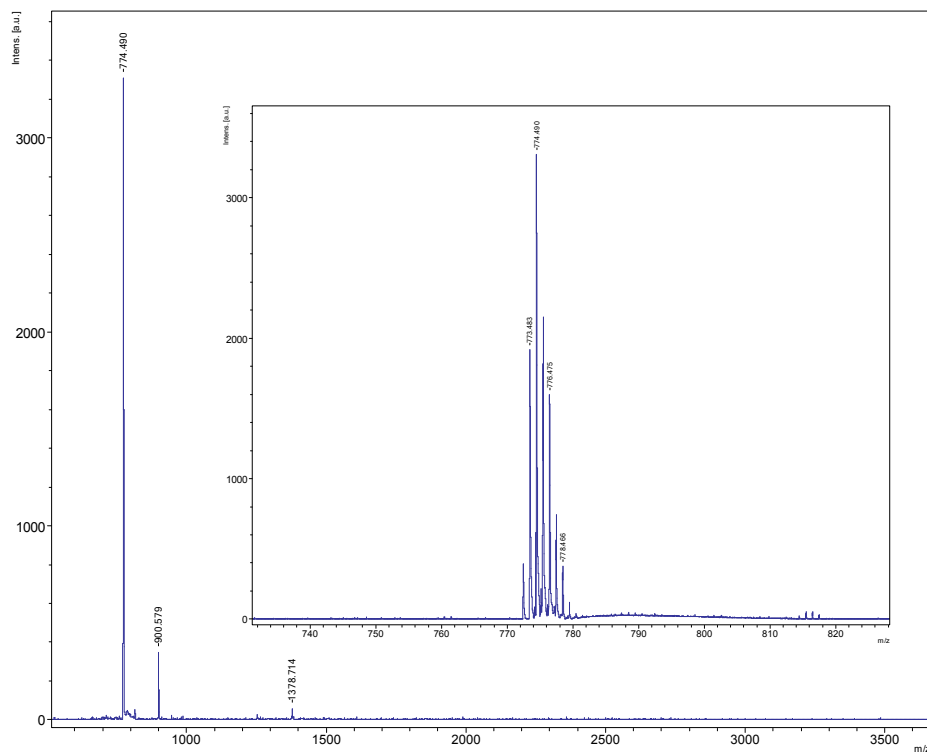
S4.1 2,2'-(4,8-bis((2-ethylhexyl)thio)benzo[1,2-b:4,5-b']dithiophene-2,6-diyl)bis(4,4,5,5-tetramethyl-1,3,2-dioxaborolane) (**10**)



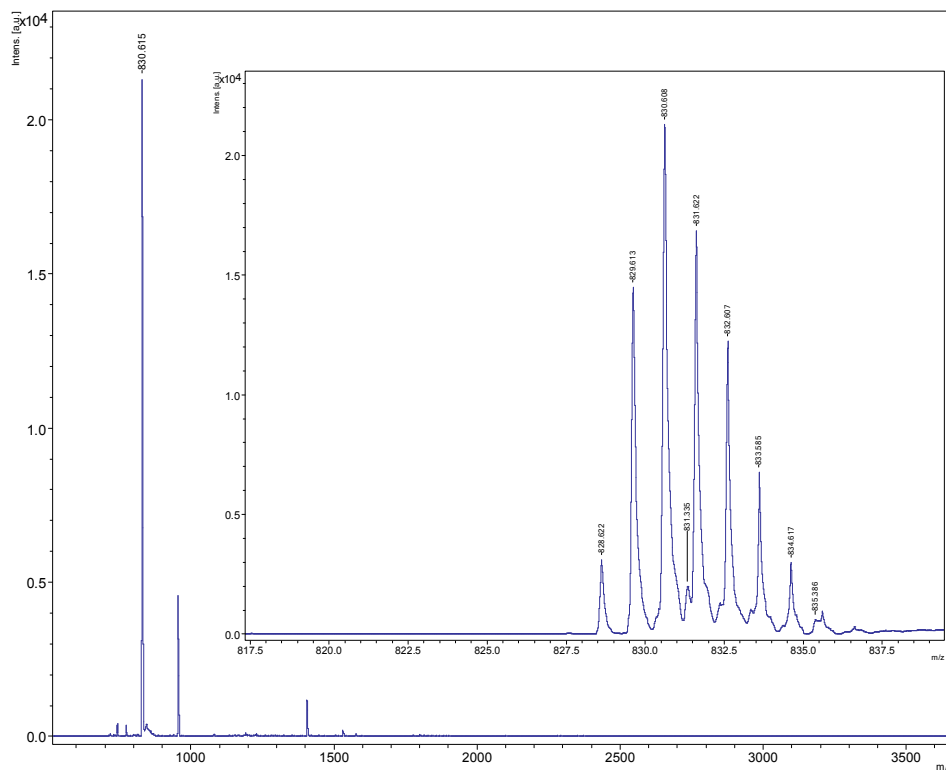
S4.2 ((2,6-bis(4,4,5,5-tetramethyl-1,3,2-dioxaborolan-2-yl)benzo[1,2-b:4,5-b']dithiophene-4,8-diyl)bis(ethyne-2,1-diyl))bis(triisopropylsilane) (**11**)



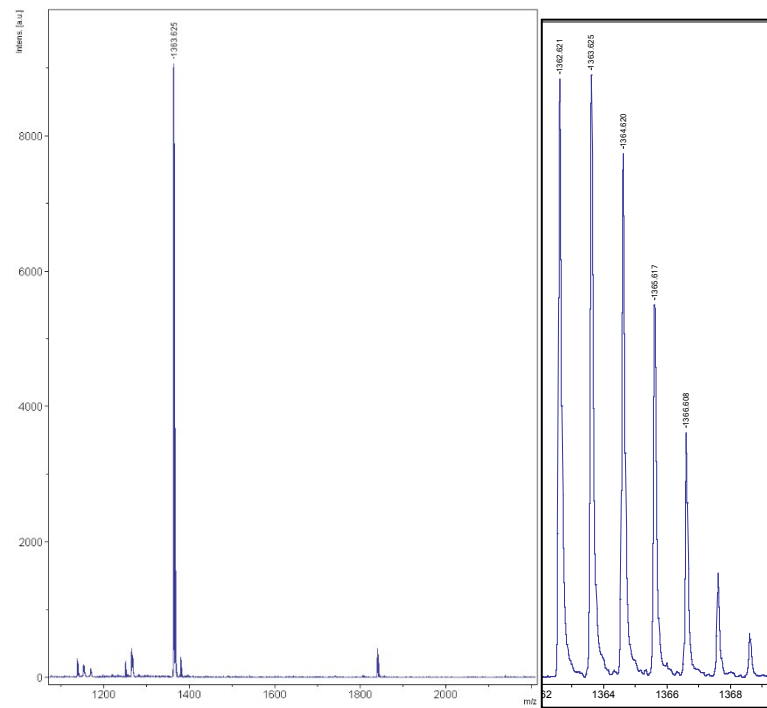
*S4.3 2,2'-(4,8-bis(5-hexylthiophen-2-yl)benzo[1,2-*b*:4,5-*b'*]dithiophene-2,6-diyl)bis(4,4,5,5-tetramethyl-1,3,2-dioxaborolane) (12)*



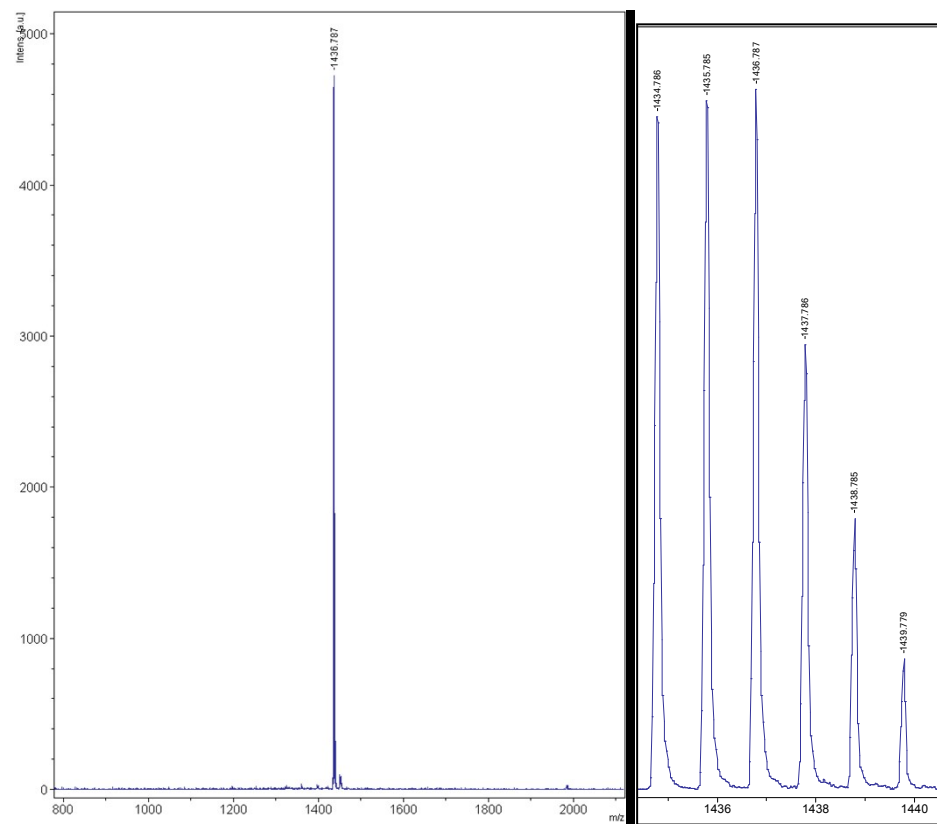
*S4.4 2,2'-(4,8-bis(5-(2-ethylhexyl)thiophen-2-yl)benzo[1,2-*b*:4,5-*b'*]dithiophene-2,6-diyl)bis(4,4,5,5-tetramethyl-1,3,2-dioxaborolane) (13)*



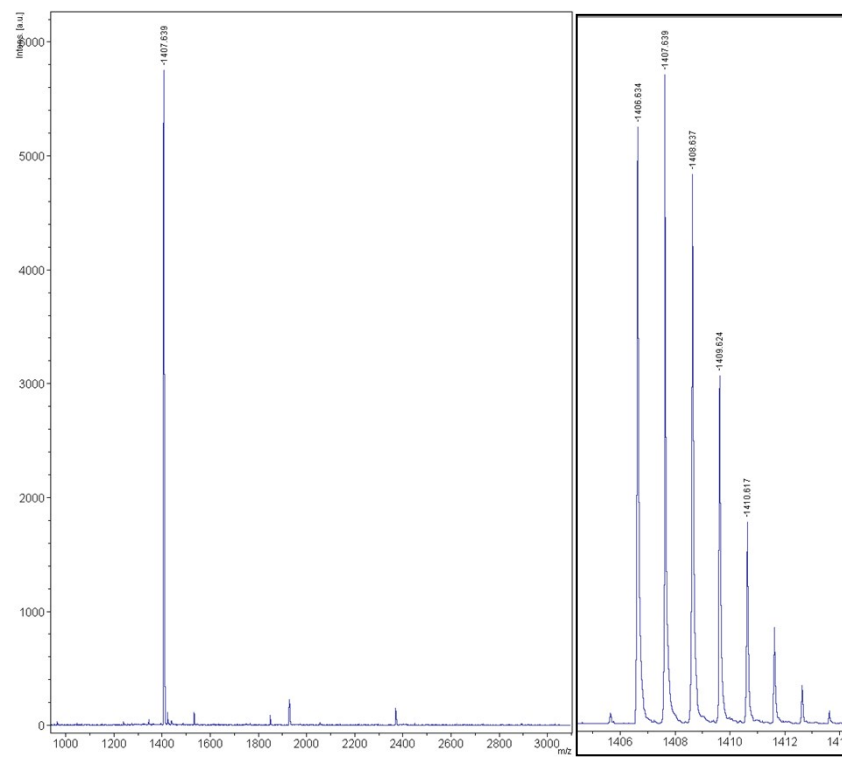
S4.5 5'',5''''-(4,8-bis((2-ethylhexyl)thio)benzo[1,2-b:4,5-b']dithiophene-2,6-diyl)bis(3',3''-dihexyl-[2,2':5',2''-terthiophene]-5-carbaldehyde) (**15**)



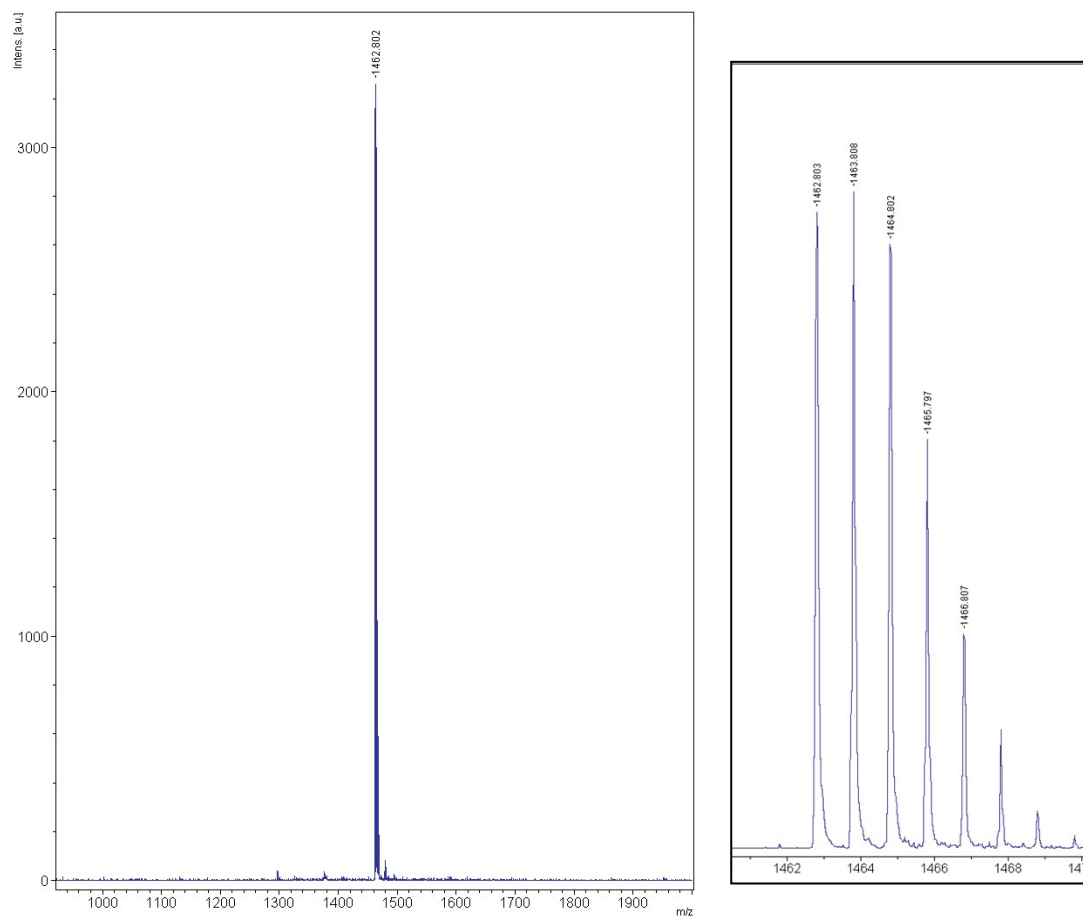
S4.6 5'',5''''-(4,8-bis((triisopropylsilyl)ethynyl)benzo[1,2-*b*:4,5-*b'*]dithiophene-2,6-diyl)bis(3',3''-dihexyl-[2,2':5',2''-terthiophene]-5-carbaldehyde) (**16**)



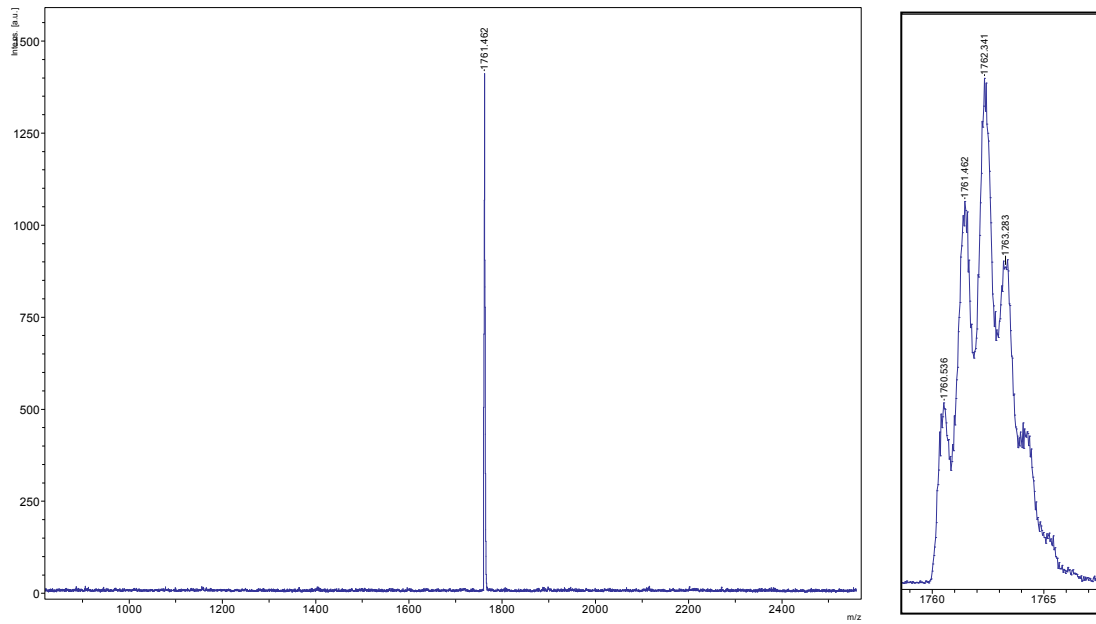
S4.7 5'',5''''-(4,8-bis(5-hexylthiophen-2-yl)benzo[1,2-b:4,5-b']dithiophene-2,6-diyl)bis(3',3''-dihexyl-[2,2':5',2''-terthiophene]-5-carbaldehyde) (**17**)



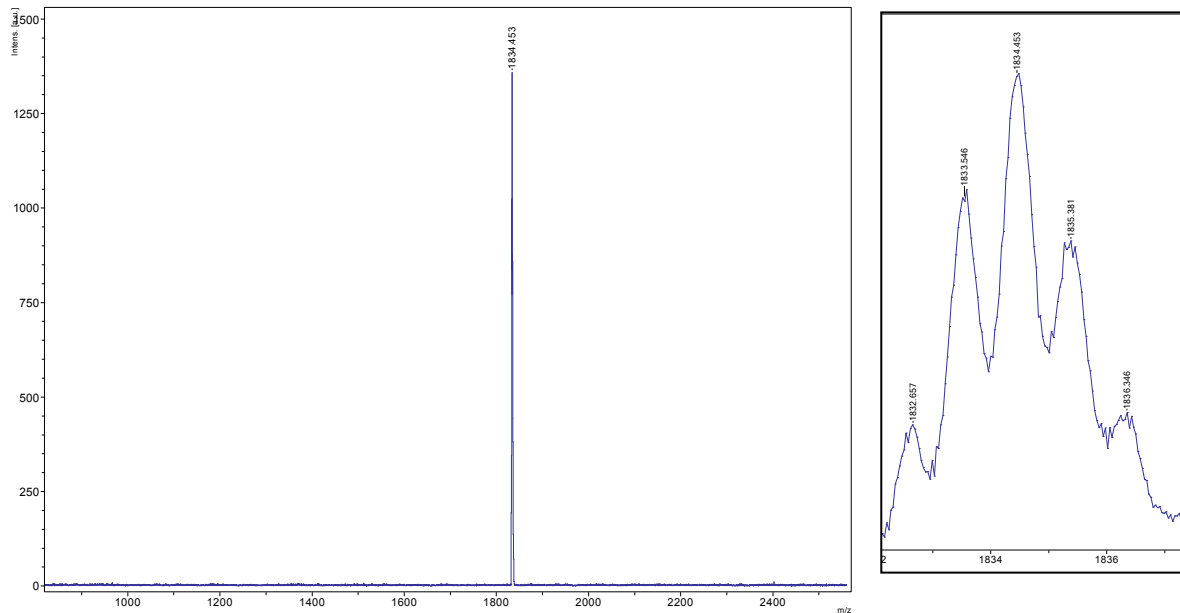
S4.8 *5'',5''''-(4,8-bis(5-(2-ethylhexyl)thiophen-2-yl)benzo[1,2-*b*:4,5-*b'*]dithiophene-2,6-diyl)bis(3',3''-dihexyl-[2,2':5',2''-terthiophene]-5-carbaldehyde) (18)*



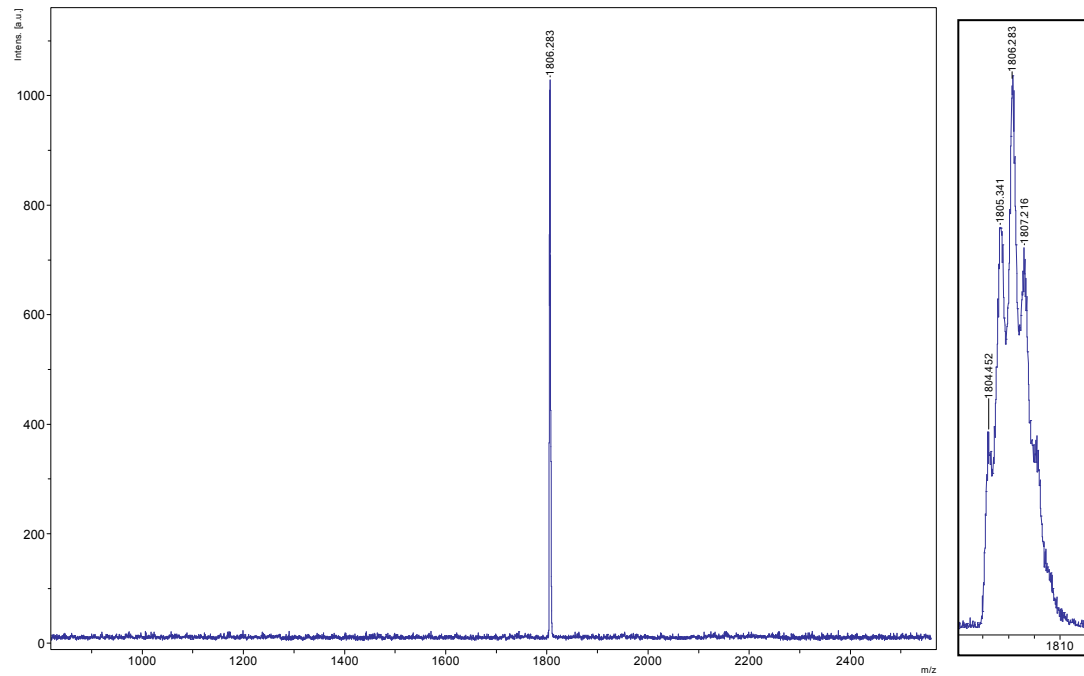
S4.9 (*(5Z,5'Z)-5,5'-((5'',5''''-(4,8-bis((2-ethylhexyl)thio)benzo[1,2-*b*:4,5-*b*']dithiophene-2,6-diyl)bis(3',3''-dihexyl-[2,2':5',2''-terthiophene]-5'',5-diyl))bis(methanylylidene))bis(3-hexyl-2-thioxothiazolidin-4-one*) (**BTR-TE**)



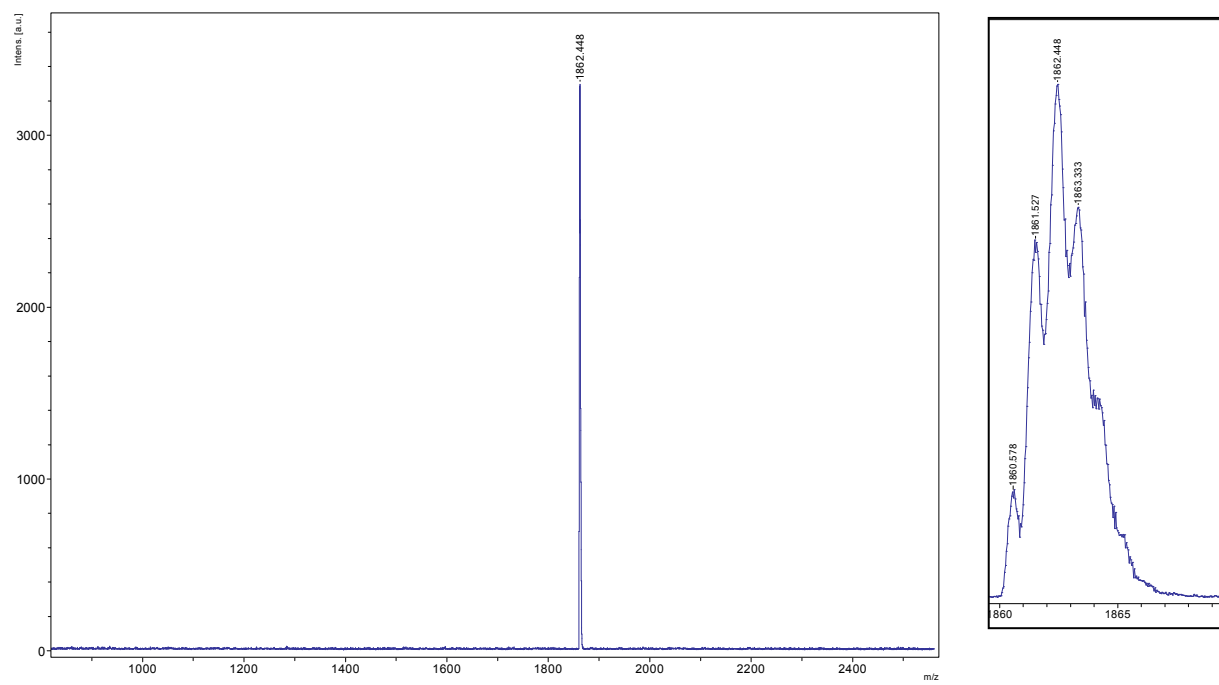
S4.10 (*(5Z,5'Z)-5,5'-((5'',5''''-(4,8-bis(triisopropylsilyl)ethynyl)benzo[1,2-*b*:4,5-*b*']dithiophene-2,6-diyl)bis(3',3''-dihexyl-[2,2':5',2''-terthiophene]-5'',5-diyl))bis(methanylylidene))bis(3-hexyl-2-thioxothiazolidin-4-one*) (**BTR-TIPS**)



S4.11 (5Z,5'Z)-5,5'-((5'',5''''-(4,8-bis(5-hexylthiophen-2-yl)benzo[1,2-b:4,5-b']dithiophene-2,6-diyl)bis(3',3''-dihexyl-[2,2':5',2''-terthiophene]-5'',5-diyl))bis(methanylylidene))bis(3-hexyl-2-thioxothiazolidin-4-one) (BTR-H)



S4.12 (5Z,5'Z)-5,5'-((5'',5''''-(4,8-bis(5-(2-ethylhexyl)thiophen-2-yl)benzo[1,2-b:4,5-b']dithiophene-2,6-diyl)bis(3',3''-dihexyl-[2,2':5',2''-terthiophene]-5'',5-diyl))bis(methanylylidene))bis(3-hexyl-2-thioxothiazolidin-4-one) (BTR-EH)



S5 Thermogravimetric Analysis Thermograms

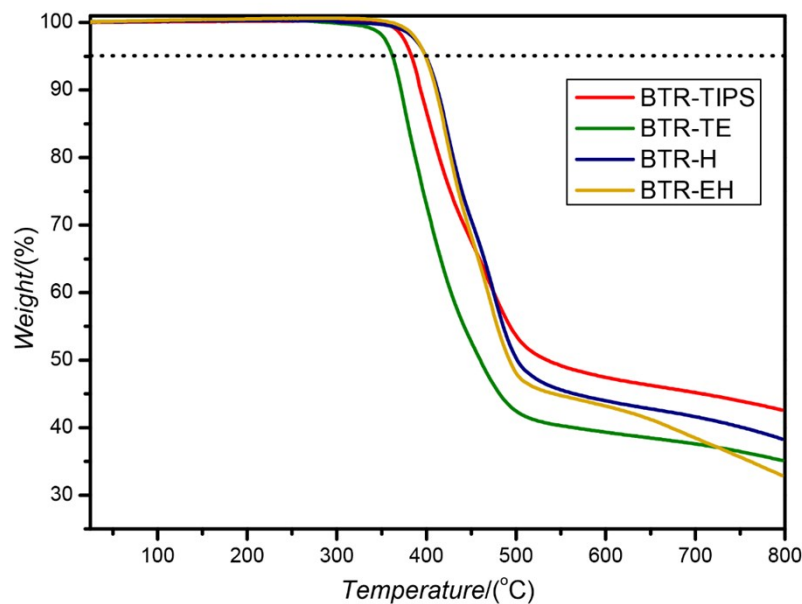


Figure S5.1. TGA thermogram for the BTR analogue materials

S6 DSC thermograms

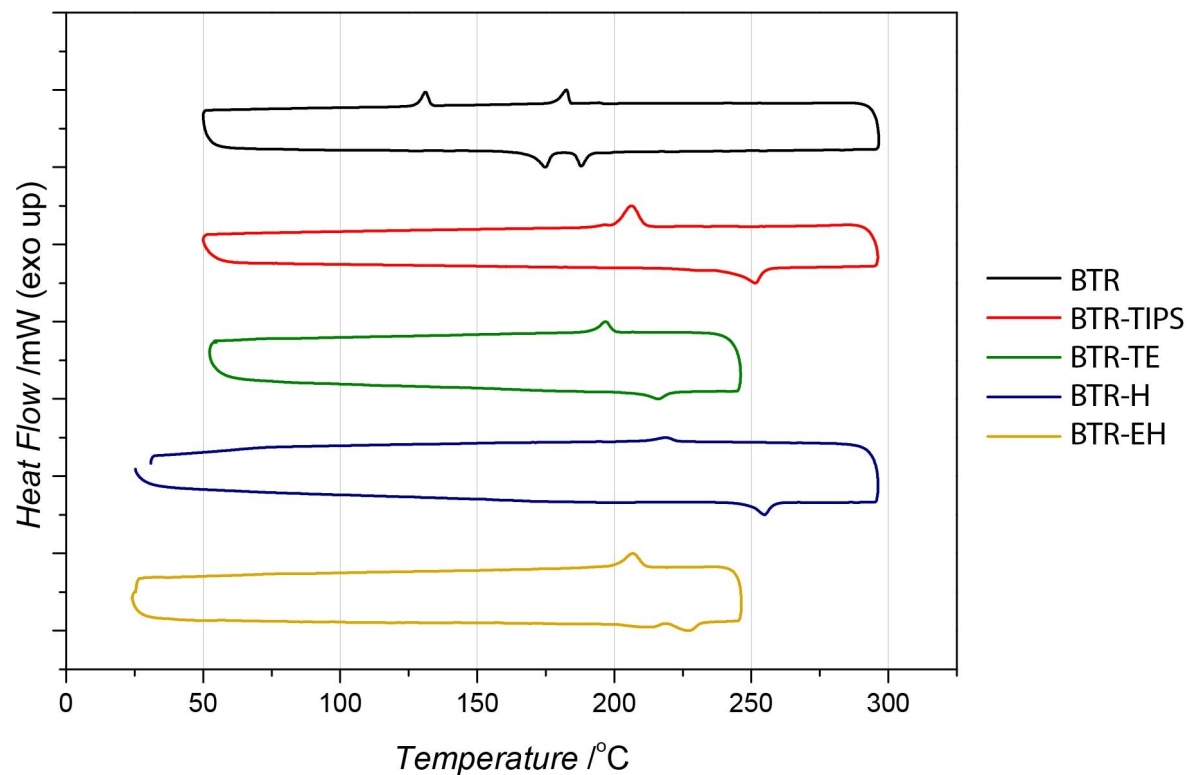


Figure S6.1. Normalized DSC thermograms for the BTR analogues.

S7 Solubility measurements

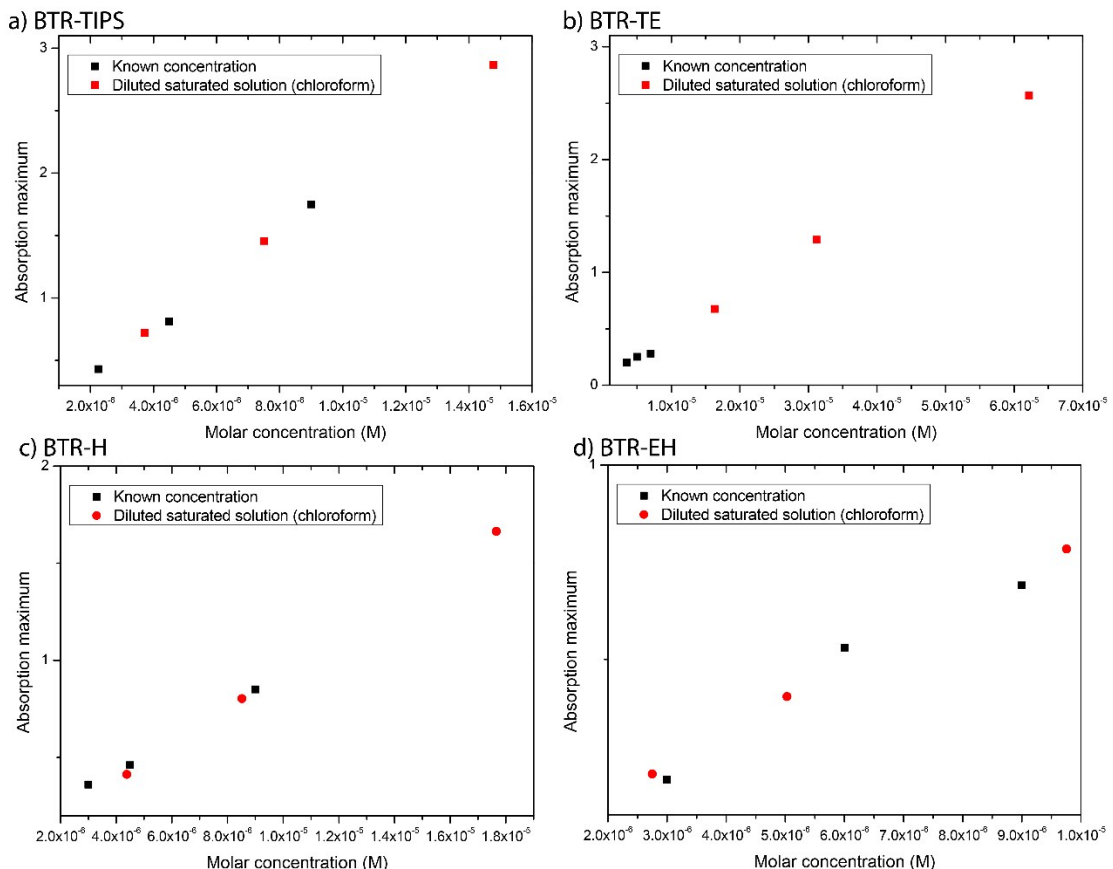


Figure S7.1. Plot of absorption maximum vs. solution concentration for a) BTR-TIPS, b) BTR-TE, c) BTR-H and d) BTR-EH analogues, allowing the derivation of solubility of the analogues in chloroform. Saturated solutions were made up, diluted by a known factor and had their absorption measured. This was compared to the maxima of solutions of known concentration.

S8 Photoluminescence spectra

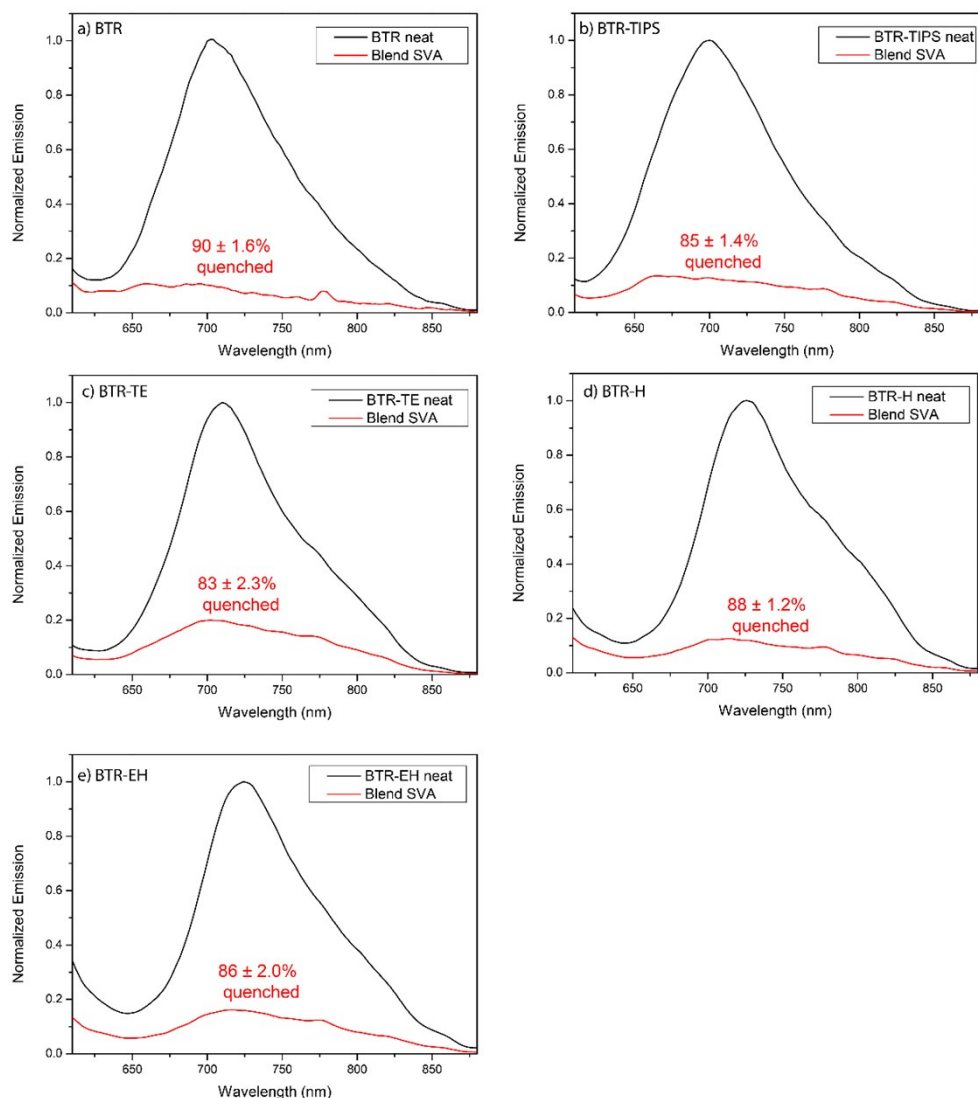


Figure S8.1. Photoluminescence spectra of a) BTR, b) BTR-TIPS, c) BTR-TE, d) BTR-H and e) BTR-EH neat films (black) and the solvent-vapor annealed blends (reds) to show quenching of emission with the introduction of PC₇₁BM. Films were excited at 580 nm and four measurements were conducted by rotating the measured film by 90° each time to gain an average intensity spectra. The fluorescence intensities are corrected for the relative absorbance at 580 nm (Abs) by dividing the emission spectra by (1x10^{-Abs}). The fluorescence quenching efficiencies are as labelled.

S9 Cyclic Voltammograms

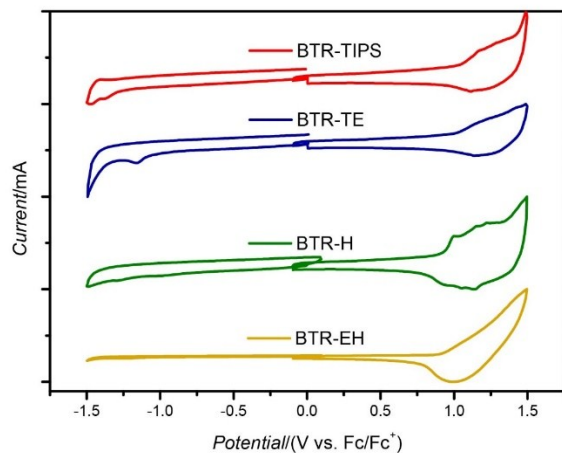


Figure S9.1. Normalized thin film cyclic voltammograms for the BTR analogues.

S10 EQE Measurements

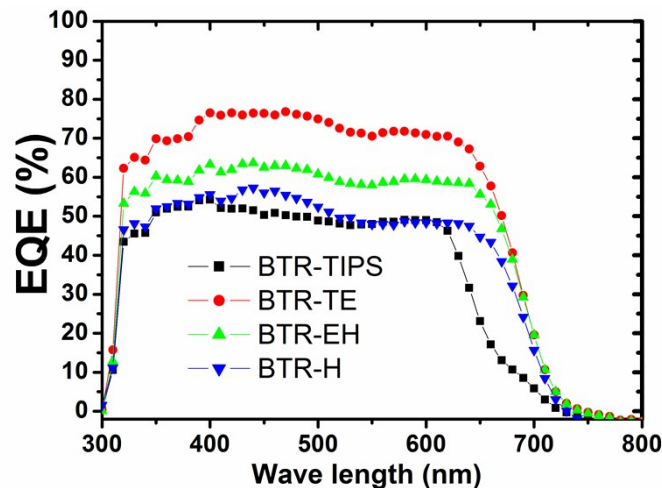


Table S1: Measured and calculated JSCs for SVA-optimized devices

Devices	Measured J _{sc} (mA/cm ²)	Calculated J _{sc} (mA/cm ²)
BTR-TIPS	8.5	8.38
BTR-TE	14	13.76
BTR-H	10.2	9.77
BTR-EH	11.9	11.61

S11 Space Charge Limited Current mobilities

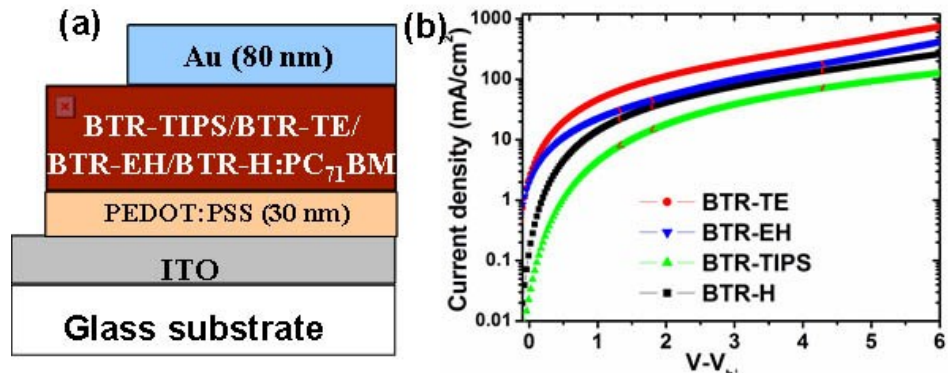


Figure S11.1 (a) Schematic diagram of hole-only device and (b) Current density-voltage curves for the hole only devices for BTR-TIPS/BTR-TE/BTE-EH/BTR-H:PC₇₁BM blends.

S12 AFM Images

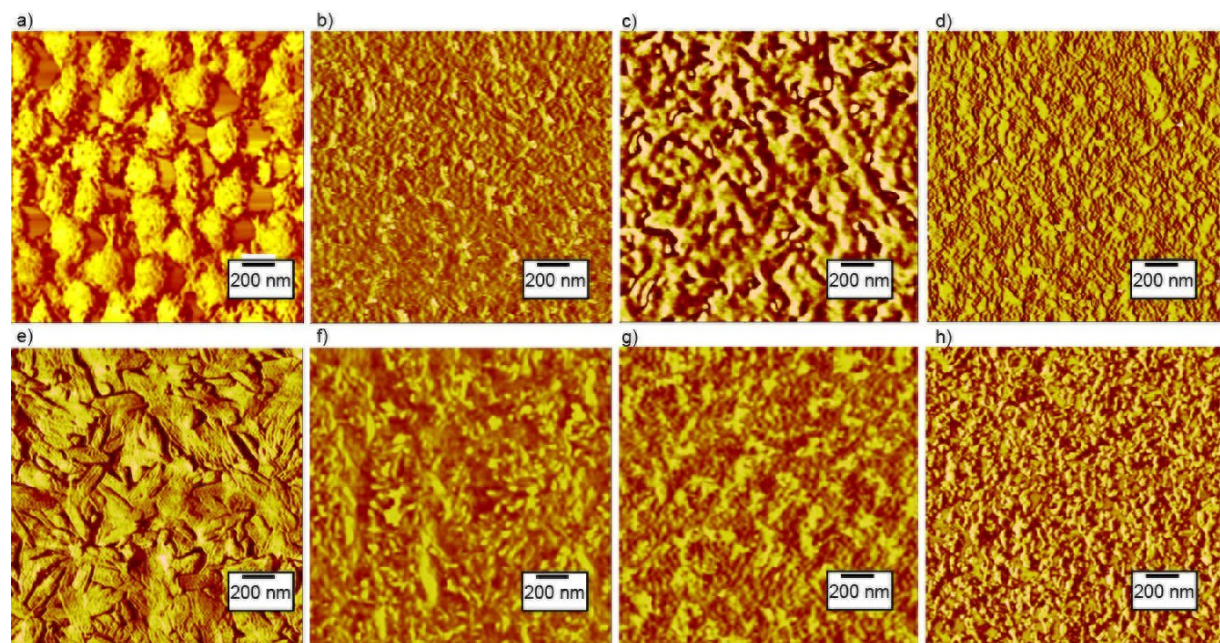
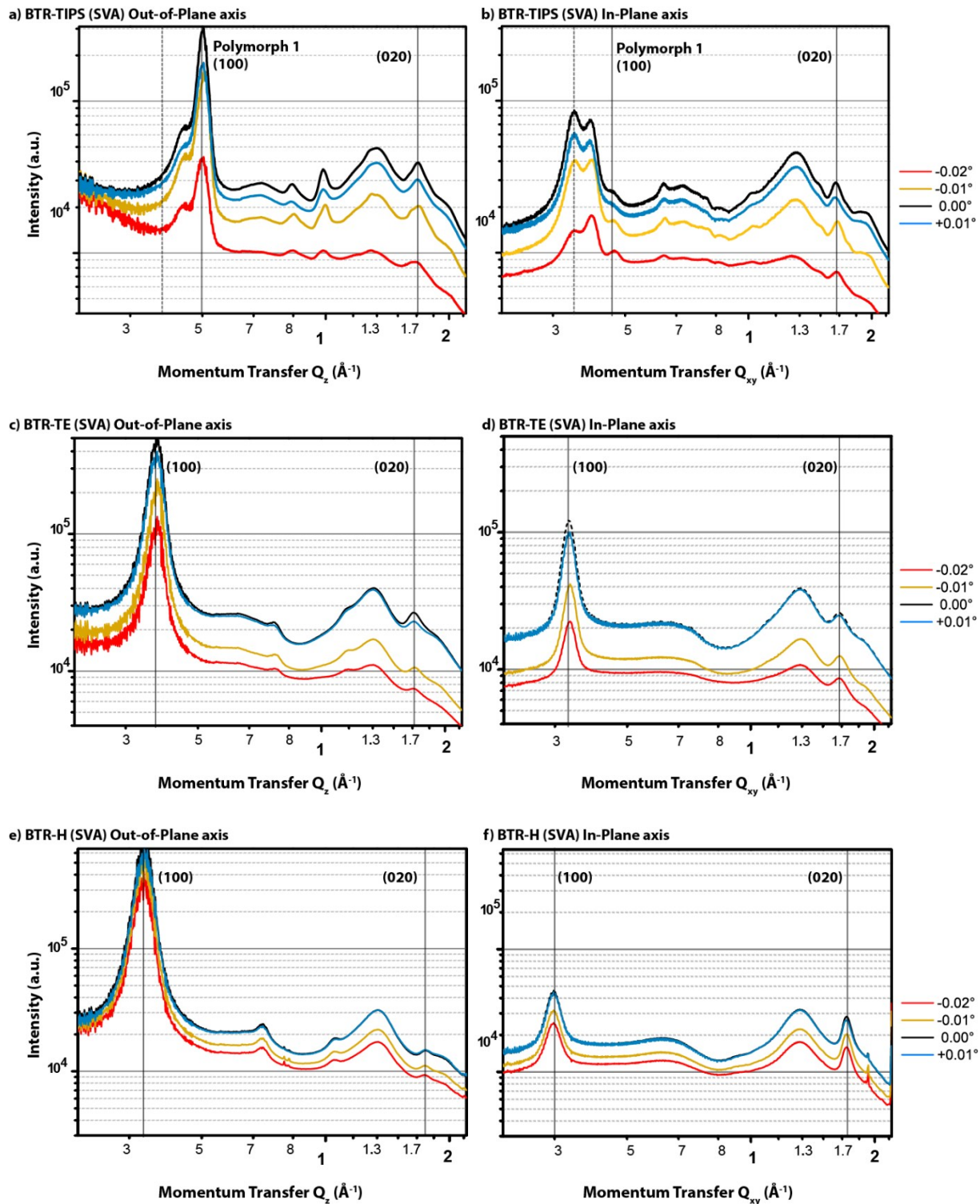


Figure S12.1. AFM images show the phase topography of an as-cast film of a 1:1 weight ratio blend of PC₇₁BM with a) BTR-TIPS, b) BTR-TE, c) BTR-H, d) BTR-EH; and solvent vapor annealed films of the same blend with e) BTR-TIPS, f) BTR-TE, g) BTR-H and h) BTR-EH.

S13 GIWAXS Depth Profiles



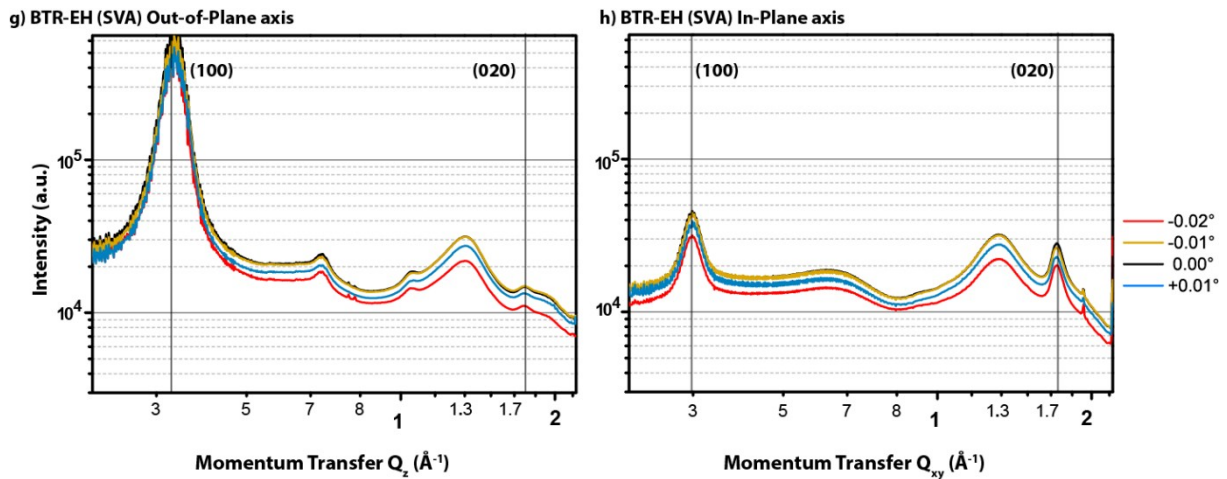


Figure S13.1. GIWAXS one-dimensional line profiles at incident angles relative to the critical angle (denoted as 0.0°) are shown in the out-of-plane and in-plane directions for **BTR-TIPS** (a-b), **BTR-TE** (c-d), **BTR-H** (e-f) and **BTR-EH** (g-h). Vertical lines are drawn to direct the eye to reflection peaks of interest, which are labelled with their unit cell indices. The dashed vertical lines for Figure S9.1a-b indicate the (100) reflection of polymorph 2 (see main text).

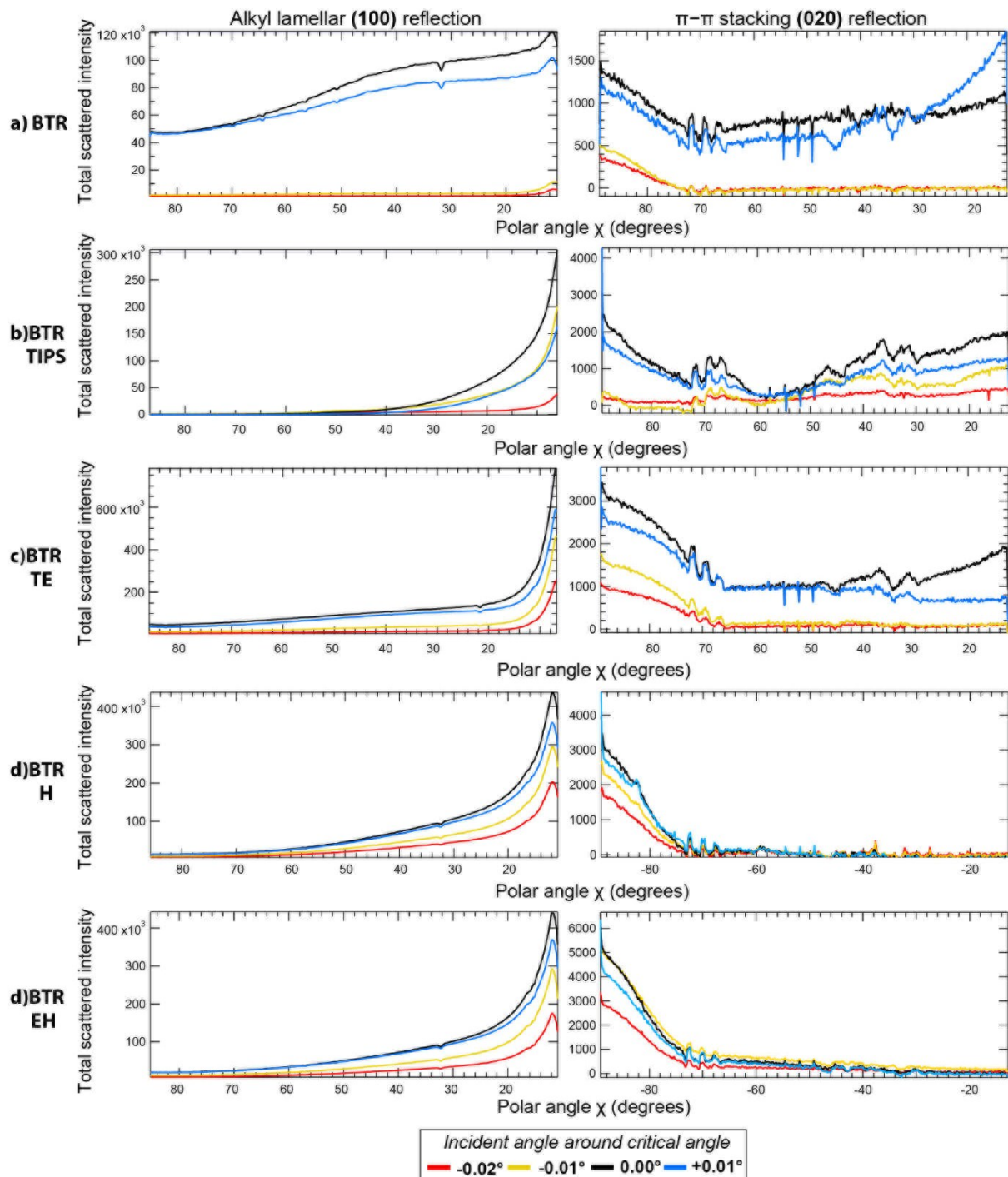


Figure S13.2. Line profiles of total scattered intensity at each polar angle of the (100) and (020) reflections taken from GIWAXS scattering patterns of a) **BTR**, b) **BTR-TIPS**, c) **BTR-TE**, d) **BTR-H** and e) **BTR-EH** at various incident angles around the critical angle. X values of 10° and 90° refer to the vertical and horizontal axes of the scattering pattern, respectively.

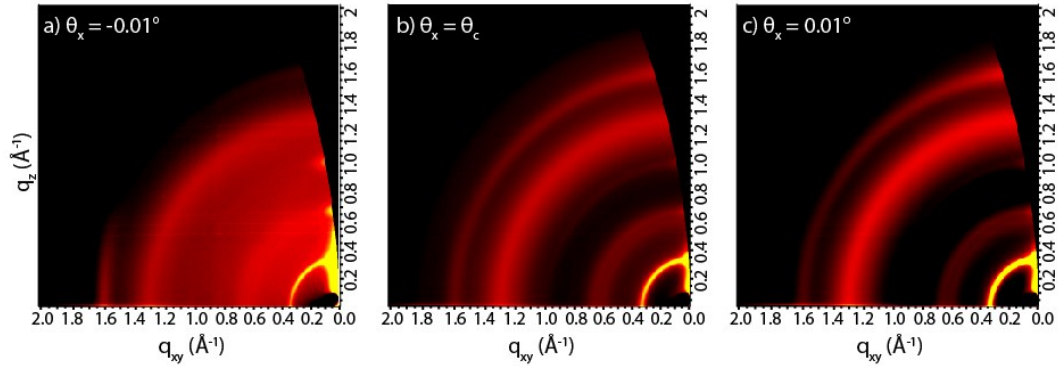


Figure S13.3. GIWAXS scattering patterns of the SVA-treated BTR:fullerene blend taken at various incident angles θ_x around the critical angle. Note the change in the [020] π -stacking reflection at $q = 1.62 \text{ \AA}^{-1}$.

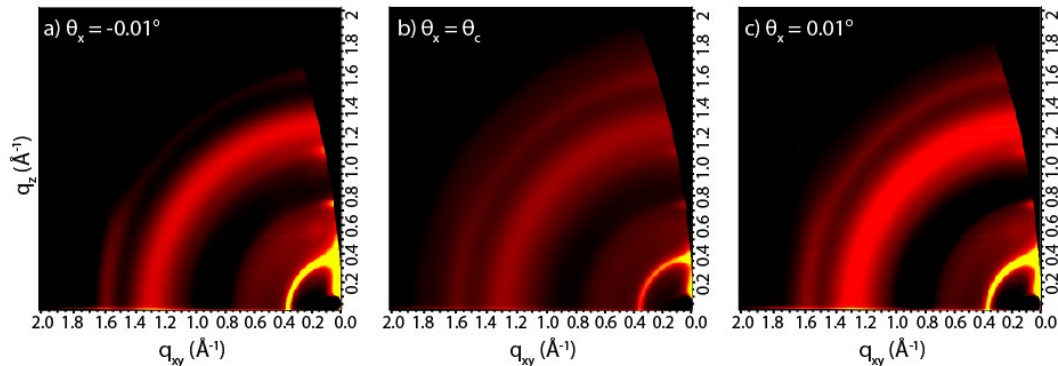
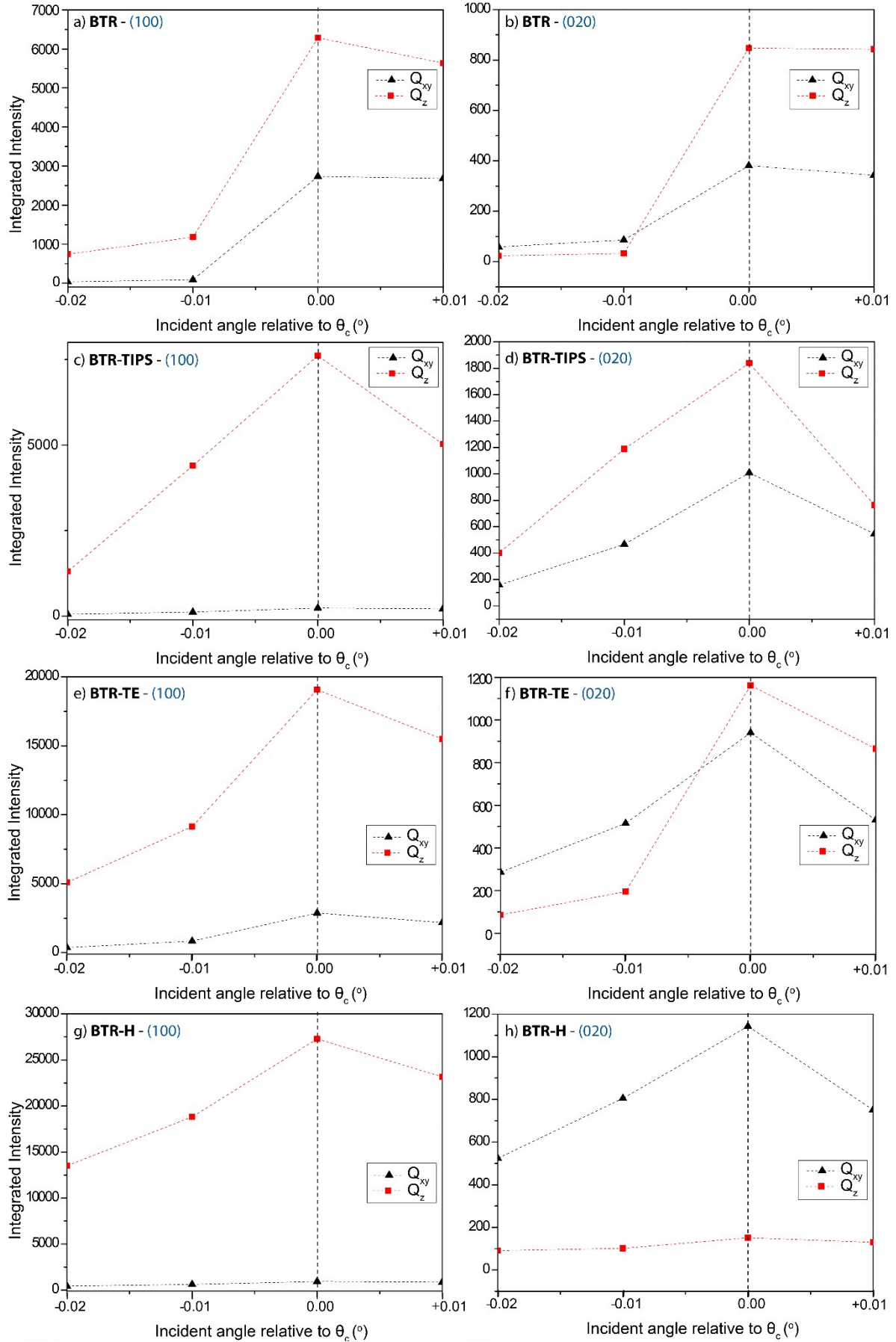


Figure S13.4. GIWAXS scattering patterns of the SVA-treated BTR-TE:fullerene blend taken at various incident angles θ_x around the critical angle. Note the change in the [020] π -stacking reflection at $q = 1.62 \text{ \AA}^{-1}$.



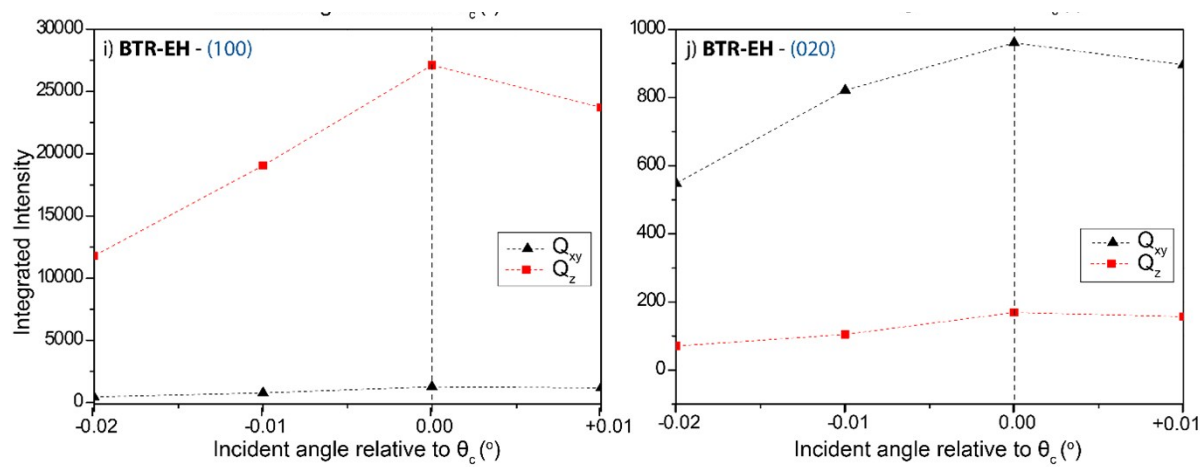
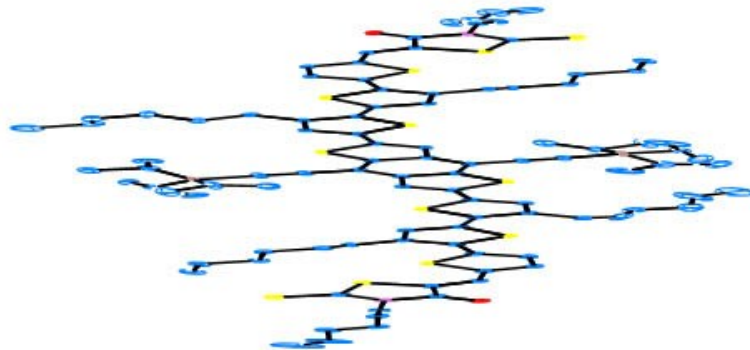


Figure S13.5. Integrated intensities of peaks corresponding to the (100) and the (020) reflections along the q_{xy} (black) and q_z (red) axes of: a-b) BTR, c-d) BTR-TIPS, e-f) BTR-TE, g-h) BTR-H and i-j) BTR-EH, against the incident angle. Peaks were determined via a Gaussian fit. Red and black dashed lines are intended to aid visualization.

S14 Crystallography



Crystal data for **BTR-TIPS**. $C_{100}H_{127}N_2 O_2S_{12}Si_2 M = 1829.93, T = 100.0(2) K, \lambda = 0.710920 \text{ \AA}$, Triclinic, space group $P-1$, $a = 15.075(3)$, $b = 17.897(4)$, $c = 20.430(4) \text{ \AA}$, $\alpha = 67.14(3)^\circ$, $\beta = 81.00(3)^\circ$, $\gamma = 77.91(3)^\circ V = 4949(2) \text{ \AA}^3$, $Z = 2$, $D_c = 1.228 \text{ Mg M}^{-3}$, $\mu = 0.337 \text{ mm}^{-1}$, $F(000) = 1954$, crystal size $0.07 \times 0.03 \times 0.005 \text{ mm}$. $\theta_{\max} = 31.79^\circ$, 83760 reflections measured, 22426 independent reflections ($R_{\text{int}} = 0.048$) the final $R = 0.0936[I > 2\sigma(I)]$, 15002 data] and $wR(F^2) = 0.2895$ (all data) GOOF = 1.039. **CCDC code:** 1864646.

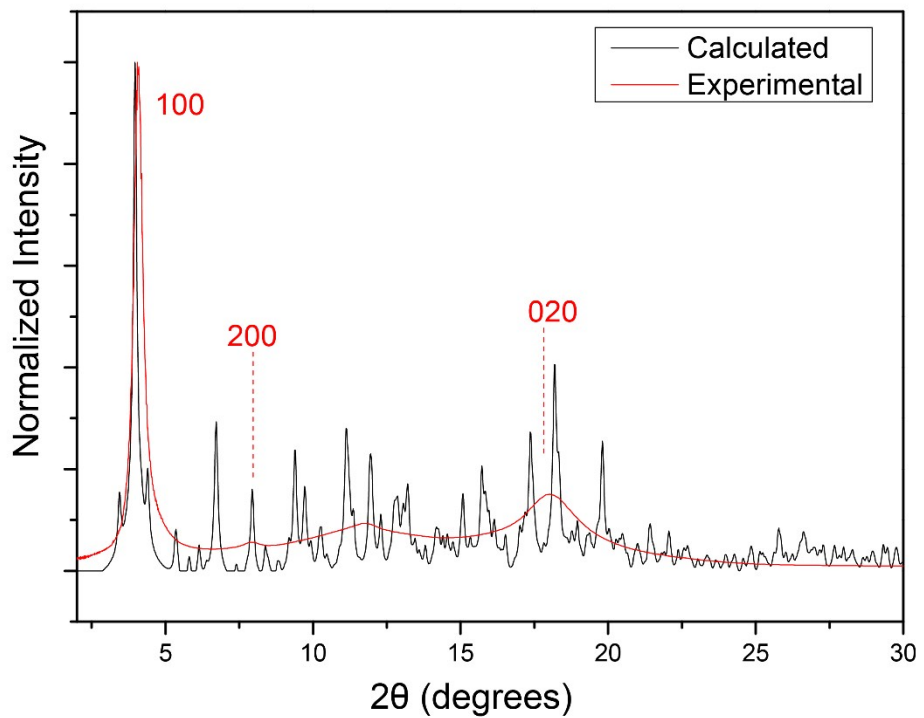


Figure S14.1. Simulated (black line) powder diffraction pattern for the BTR-TIPS structure derived from the single-crystal (CCDC code: 1864646) and experimentally-determined GIWAXS linecut (red line) of a neat, as-cast film. Wavelength used for calculations: 1.12713 Å